(pCr) to ADP to yield ATP and creatine and is known to play important roles in local delivery and cellular compartmentalization of ATP (48, 51). The findings obtained here suggest that recruitment of CKB to the HCV RC, through CKB interaction with NS4A, is essential for maintenance or enhancement of viral replicase activity.

MATERIALS AND METHODS

Cell lines, antibodies, and reagents. Human hepatoma cell line Huh-7.5.1 (54) was kindly provided by Francis V. Chisari. Cell lines carrying subgenomic replicon RNAs, namely, SGR-N (41) and SGR-JFH1 (23), were derived from the HCV-N (17) and JFH-1 strains (24), respectively. Mouse monoclonal antibodies (MAbs) against HCV NS3 (Chemicon, Temecula, CA), NS4A (Santa Cruz Biotechnology, Inc., Santa Cruz, CA), NS5A (Biodesign, Saco, ME), NS5B (2), FLAG (M2; Sigma-Aldrich, St. Louis, MO), glyceraldehyde-3-phosphate dehydrogenase (GAPDH; Chemicon), and Flotillin-1 (BD Biosciences, San Jose, CA) and polyclonal antibodies (PAbs) against CKB (mouse [Abnova, Taipei, Taiwan], goat [Santa Cruz]), hemagglutinin (HA; Sigma-Aldrich), and FLAG (Sigma-Aldrich) were used. Cyclocreatine (Ccr; also known as 2-imino-1-imidazolidineacetic acid), pCr, and phosphopyruvic acid (pPy) were purchased from Sigma-Aldrich. Recombinant CKB and pyruvate kinase (PK) were obtained from Acris (Herfold, Germany) and Calbiochem (San Diego, CA), respectively.

Proteome analysis. RC-rich membrane fractions of cells were isolated as described previously (2, 41). Briefly, cells were lysed in hypotonic buffer. After removing the nuclei, supernatants were treated with 1% NP-40 for 60 min, mixed with 70% sucrose, overlaid with 55 and 10% sucrose, and centrifuged at 38,000 rpm for 14 h. Proteins from membrane fractions were purified by using a 2D Clean-Up kit (GE Healthcare, Tokyo, Japan), followed by labeling with fluorescent dyes: Cy5 for replicon cells, Cy3 for parental cells, and Cy2 for the protein standard containing equal amounts of both cell samples. Two-dimensional fluorescence difference gel electrophoresis (2D-DIGE) was performed using Immobiline DryStrip as the first-dimension gel and 12.5% polyacrylamide gel as the second-dimension gel. The 2D-DIGE images were analyzed quantitatively using the DeCyder software (GE Healthcare). Student *t* test was performed on differences between the tested samples using DeCyder biological variation analysis module. Samples were analyzed in triplicate. The protein spots of interest were excised from the gel, subjected to in-gel digestion using trypsin or lysyl endopeptidase and analyzed by liquid chromatography (MAGIC 2002 System; Michrom Bioresources, Auburn, CA) directly connected to electrospray ionization-ion trap mass spectrometry (LCQ-decaXP; Thermo Electron Corp., Iwakura, Japan). The results were subjected to database (NCBInr) search by Mascot server software (Matrix Science, Boston, MA) for peptide assignment.

Plasmids. A human CKB cDNA (43; kindly provided by Oriental Yeast Corp., Tokyo, Japan) was inserted into the EcoRI site of pCAGGS, yielding pCAGCKB. To generate expression plasmids for HA-tagged versions of wild-type and deletion mutated CKB, the corresponding DNA fragments were amplified by PCR, followed by introduction into the BglII site of pCAGGS. A fragment representing the inactive mutant CKB-C283S was synthesized by PCR mutagenesis. To generate FLAG-tagged NS protein expression plasmids, DNA fragments encoding either NS3, NS4A, NS4B, NS5A, or NS5B protein were amplified from HCV strains NIHJ1 (1) and JFH-1 (23) by PCR, followed by cloning into the EcoRI-EcoRV sites of pcDNA3-MEF (20). To generate an HA-tagged NS3 expression plasmid, a fragment encoding NS3 with the HA tag sequence at its N terminus was inserted into pCAGGS.

siRNA transfection. The small interfering RNAs (siRNAs) targeted to CKB (CKB-1 [5′-UAAGACCUUCCUGGUGUGGTT-3′] and CKB-2 [5′-CGUCAC CCUUGGUAGAGUUTT-3′]) and the scramble negative control siRNA to CKB-2 (5′-GGCGUACUAGCUUAUUCGCTT-3′) were purchased from Sigma. Cells in a 24-well plate were transfected with siRNA using HiPerFect transfection reagent (Qiagen, Tokyo, Japan) according to the manufacturer's instructions. The siRNA sequences for the other genes used in the siRNA screening are available upon request.

HCV infection. Culture media from Huh-7 cells transfected with in vitro-transcribed RNA corresponding to the full-length JFH-1 (47) was collected, concentrated, and used for the infection assay (3).

Quantification of HCV core protein and RNA. To estimate the levels of HCV core protein, aliquots of culture supernatants or of cell lysates were assayed by using HCV Core enzyme-linked immunosorbent assay kits (5). Total RNA was isolated from harvested cells using TRIzol (Invitrogen, Carlsbad, CA). Copy numbers of the viral RNA were determined by reverse transcription-PCR (RT-PCR) (2, 36, 46).

Immunoprecipitation, immunoblot analysis, and immunofluorescence microscopy. The analyses, as well as DNA transfection, were performed essentially as previously described (42). Cells were lysed in immunoprecipitation lysis buffer (50 mM Tris-HCl [pH 7.6], 150 mM NaCl, 1% sodium deoxycholate, 1% NP-40, 0.1% sodium dodecyl sulfate, 1 mM dithiothreitol, 1 mM calcium acetate). For immunoprecipitation, supernatants of cell lysates were precipitated with anti-FLAG antibody and protein A-Sepharose Fast Flow beads (GE healthcare). For immunofluorescence microscopy, anti-CKB goat PAb and anti-NS4A MAb as primary antibodies and Alexa Fluor 555-conjugated donkey anti-goat immunoglobulin G (Invitrogen) and Alexa Fluor 488-conjugated rabbit anti-mouse immunoglobulin G (Invitrogen) as secondary antibodies were used and observed under an LSM 510 confocal microscope (Carl Zeiss, Oberkochen, Germany).

Immunoelectron microscopy. Postembedding immunostaining using the colloidal gold-labeling method was performed as described previously (38). Cells were fixed in 4% paraformaldehyde–1% glutaraldehyde at 4°C for 1 h. After dehydration through a graded series of ethanol, cells were embedded in LR White (London Resin Company, London, United Kingdom) and sectioned. After blocking, section grids were incubated with a mixture of anti-NS4A and anti-CKB antibodies at 4°C overnight, followed by treatment with a mixture of 18-nm colloidal gold-conjugated donkey anti-mouse immunoglobulin G and 12-nm colloidal gold-conjugated donkey anti-goat immunoglobulin G antibodies (Jackson Immunoresearch, West Grove, PA) at 4°C overnight. The sections were stained with uranyl acetate and observed under a transmission electron microscope.

Measurement of CK activity and cellular ATP level. Cells were lysed with passive lysis buffer (Promega, Madison, WI), and CK activities were measured based on Oliver methods (40), in which the activity of converting creatine phosphate and ADP to creatine and ATP was measured. ATP levels in cell lysates were measured by using a CellTiter-Glo luminescent cell viability assay (Promega).

RNA replication assays in permeabilized replicon cells and in vitro. The RNA synthesis assay using permeabilized replicon cells was based on a previously described method (33). Briefly, SGR-JFH1 cells were treated with 5 μg of actinomycin D/ml for 2 h, followed by permeabilization with 50 μg of digitonin/ml for 5 min. The resulting mix was incubated with 500 μM concentrations of ATP, GTP, and CTP; 10 μCi of UTP ([α-^{32}P]UTP); 50 μg of actinomycin D/ml; and 5 mM pCr with or without 20 U of CKB/ml for 4 h at 27°C. RNA was extracted by using TRIzol and analyzed by 1% formaldehyde agarose gel electrophoresis. The cell-free RNA replication assay was performed as described previously (2).

In vitro helicase assays. Helicase activity on double-stranded RNA (dsRNA) was investigated as described previously (11) with some modifications. The 5′ end of the release strand was labeled with [γ-^{32}P]ATP using T4 polynucleotide kinase (Ambion). The dsRNA substrate was obtained by annealing the labeled RNA with a template strand RNA at a molar ratio of 1:1. The helicase assay mixture contained 5 nM dsRNA, helicase enzyme (80 nM NS3 or NS3-4A [kindly provided by R. De Francesco]), 6 mM ATP, in the presence or absence of 20 U of CKB/ml in an assay buffer (25 mM MOPS-NaOH [pH 7.0], 2.5 mM dithiothreitol, 100 μg of bovine serum albumin/ml, 3 mM $MgCl_2$, 5 mM pCr, 2.5 U of RNase inhibitor/ml). After the helicase reaction, samples were electrophoresed in a native 8% polyacrylamide gel and autoradiographed.

To determine the effect of PK/pPy system on the helicase activity, PK and pPy were used instead of CKB and pCr. Helicase activity on dsDNA was measured based on homogeneous time-resolved fluorescence quenching using a Trupoint helicase assay kit (Perkin-Elmer, Waltham, MA) according to the manufacturer's instructions.

In vitro protease assay. In vitro HCV protease activity of NS3-4A or NS3 was analyzed by using a SensoLyteHCV protease assay kit (AnaSpec, San Jose, CA) according to the manufacturer's instructions.

RESULTS

Identification of host factors involved in HCV RNA replication by comparative proteomic analysis of DRM fractions and RNAi silencing. To identify host proteins involved in the HCV RC, proteome profiles of the RC-rich membrane fraction in Huh-7 cells harboring subgenomic replicon RNA derived from genotype 1b, N isolate (SGR-N) were compared to those of parental cells by 2D-DIGE. We confirmed that the DRM fraction obtained from SGR-N cells is functionally active in a

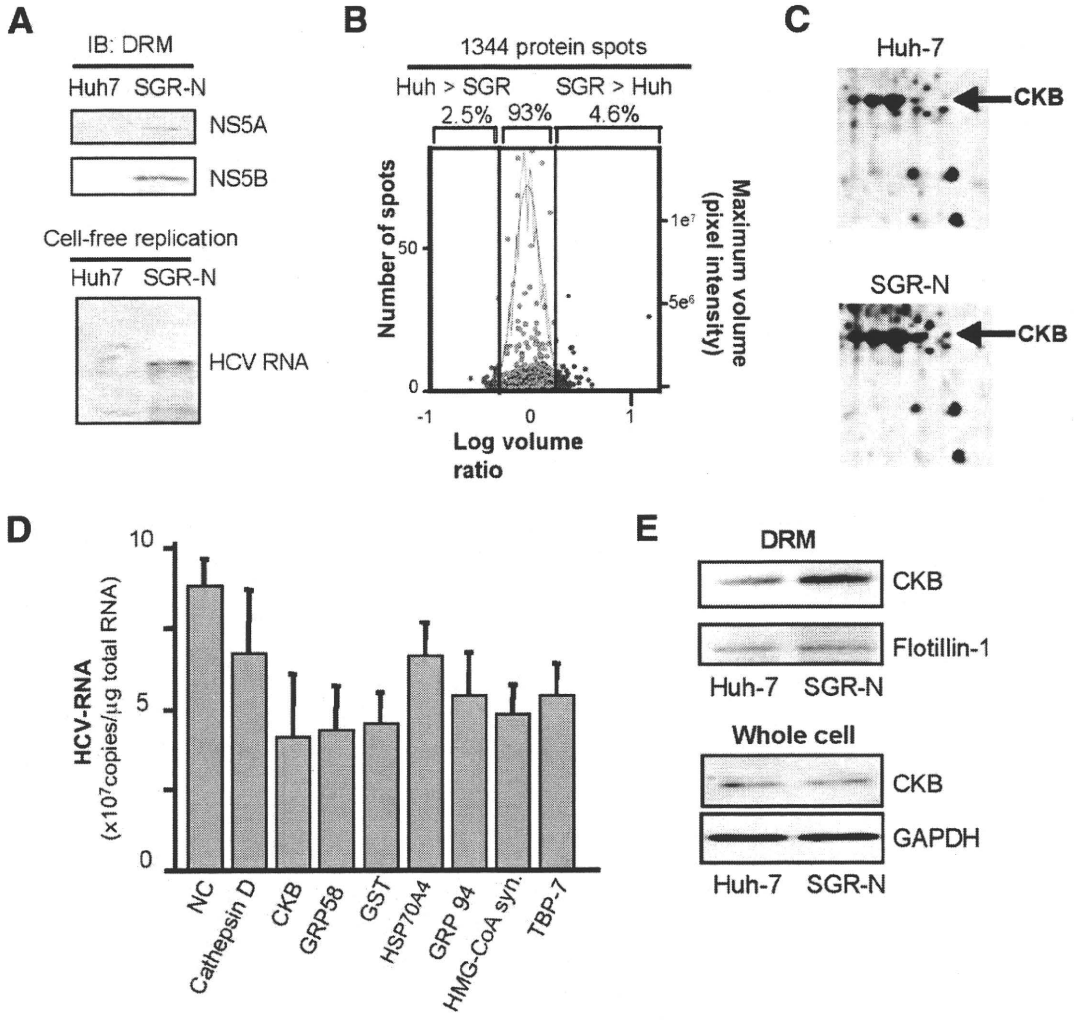

FIG. 1. Comparative proteomic analysis of DRM fractions and RNAi silencing. (A) Preparation of functionally active RC fraction for proteome analysis. DRM fractions obtained from SGR-N cells and parental Huh-7 cells were analyzed by immunoblotting with anti-NS5A and anti-NS5B antibodies (upper panel) and by the cell-free RNA replication assay (lower panel). (B) Histogram representation of proteins detected in 2D-DIGE. Images were analyzed quantitatively by the DeCyder software. The left and right *y* axis, respectively, indicate the spot frequency and the maximum volume of each spot, given against the log volume ratio (*x* axis). (C) Comparison of 2D-DIGE maps of proteins from DRM fractions of SGR-N cells and Huh-7 cells. Enlarged 2D-DIGE gel images of regions containing protein spots of CKB (arrows) are shown. (D) Effects of siRNAs of genes selected from comparative proteome analysis on HCV RNA replication. SGR-N cells were transfected with siRNA specific to cathepsin D, CKB (siCKB-1), GRP58, GST, Hsp70 protein 4, GRP94, HMG-coenzyme A synthase, or Tat binding protein 7 or with nontargeting (NC) siRNA. At 48 h posttransfection, total RNA was isolated and HCV RNA levels were assessed by real-time RT-PCR. (E) Enrichment of CKB in the DRM of HCV replicon cells. Equal amounts of DRM fractions from SGR-N and parental Huh-7 cells, or whole-cell lysates from both cells were analyzed by immunoblotting with antibodies against CKB, flotilin-1 or GAPDH.

cell-free replication assay (Fig. 1A). Three independent proteome experiments were performed for a reliable analysis of protein expression. Approximately 1,300 spots were resolved in each gel, and 4 to 5% of the protein spots represented a >2-fold increase in the membrane fraction of replicon cells in each experiment (Fig. 1B). The protein spots that exhibited high reproducibility (an example shown in Fig. 1C) were excised, digested by trypsin or lysyl endopeptidase, and analyzed by mass spectrometry, which identified the corresponding proteins in 27 cases (Table 1). Among the proteins implicated in a variety of functional categories, 10 were involved in protein folding, mainly as chaperones, 7 were metabolic and biosynthesis enzymes including proteins for redox regulation or energy pathways, 3 were involved in cytoskeleton organization, and 3 proteins were related to cellular processes, mainly proteolysis pathways. The viral NS proteins identified as differentially expressed proteins in the analysis were not listed.

In order to identify host factors involved in HCV replication, we examined the effects on viral RNA replication of transfection of SGR-N cells with siRNAs against genes encoding nine proteins belonging to diverse classes of biological functions (Table 1). Each siRNA reduced the HCV RNA level to 47 to 76% of the level of the siRNA control (Fig. 1D). None of the siRNAs tested exhibited considerable cytotoxicity against the replicon cells, ruling out overt toxicity as a mechanism for inhibition of viral RNA replication. Among the candidate

TABLE 1. Selected proteins that reproducibly increased in the DRM fraction of SGR-N cells[a]

Avg ratio	*P* (Student *t* test)	Coverage (%)	Protein name	Molecular function	GI no.
5.56	0.04	27	GRP94	Protein folding	15010550
4.99	0.07	47	Hsp60	Protein folding	6996447
3.73	0.07	6	tRNA guanine transglycosylase	Metabolism	30583205
3.56	0.06	23	KIAA0088	Unknown	577295
3.32	0.07	4	Thioredoxin-related protein	Unknown	20067392
3.32	0.13	12	Tat binding protein 1 (TBP-1)	Cellular processes	20532406
3.06	0.14	22	Aldehyde dehydrogenase 1	Metabolism	2183299
3.06	0.14	14	Chaperonin TRiC/CCT, subunit 2	Protein folding	54696794
2.96	0.04	14	Heat shock 70-kDa protein 4 (HSPA4)	Protein folding	6226869
2.96	0.04	29	GRP58	Metabolism/protein folding	2245365
2.94	0.01	37	Mutant β-actin	Cytoskeleton organization	28336
2.65	0.17	33	Glutathione S-transferase (GST)	Catalytic activity	2204207
2.53	0.04	37	Keratin 19	Cytoskeleton organization	6729681
2.46	0.08	6	Heterogeneous nuclear ribonucleoprotein K	Nucleic acid modification	460789
2.45	0.001	13	HMG-coenzyme A synthase	Metabolism	30009
2.4	0.02	31	CKB	Energy pathway/metabolism	180570
2.4	0.02	11	Cathepsin D	Cellular processes	30582659
2.4	0.02	11	C8orf2	Unknown	37181322
2.36	0.1	38	Tropomyosin 4-anaplastic lymphoma kinase fusion protein	Cytoskeleton organization	14010354
2.36	0.1	6	Calreticulin	Protein folding	30583735
2.33	0.01	29	Quinolinate phosphoribosyltransferase	Metabolism	30583301
2.29	0.04	25	Protein disulfide isomerase-related protein 5	Protein folding	1710248
2.29	0.04	16	Tat binding protein 7 (TBP-7)	Cellular processes	263099
2.05	0.11	24	Calumenin	Metabolism	2809324
2.05	0.12	10	TRiC/CCT, subunit 5	Protein folding	24307939
2.03	0.07	20	Hsp90 beta	Protein folding	34304590
2.01	0.07	10	TRiC/CCT, subunit 1	Protein folding	36796

[a] The spectra obtained by tandem mass spectrometry were collected using data-dependent mode, and the results were subjected to database (NCBInr) search by Mascot server software (Matrix Science, London, United Kingdom) for peptide assignment. Coverage, the ratio of the portion of protein sequence covered by matched peptides to the whole protein sequence. GI no., GenInfo identifier number.

genes examined, we observed a reproducible inhibition of HCV RNA replication by two independent siRNAs targeting CKB (see below).

CKB participates in HCV RNA replication and the propagation of infectious virus. CKB is a brain-type creatine kinase isoenzyme and is also detected in a variety of other tissues, including human liver (32). Steady-state levels of CKB in the DRM fraction, as well as in whole-cell lysate of SGR-N cells were compared to those from parental cells by Western blotting. The CKB level in the DRM fraction of replicon cells was higher than that in parental cells (Fig. 1E), confirming the results of the proteome analysis described above. In contrast, the CKB level in whole cells was similar in both cells (Fig. 1E). These results suggest participation of posttranslational modification, such as translocation to the DRM fraction, of CKB in replicon cells.

Figure 2A shows the inhibitory effect on HCV RNA replication of CKB siRNA; siCKB-2, the sequence of which does not overlap with the sequence of siCKB-1 used in the above siRNA screening (Fig. 1D). Transfection with siCKB-2 effectively decreased the cellular level of CKB enzymatic activity (data not shown), as well as the abundance of CKB protein (Fig. 2A), and resulted in 60% reduction in the viral RNA level in SGR-N cells compared to the cells treated with control siRNA. This inhibitory effect of siRNA on HCV RNA abundance was also observed in JFH-1-derived subgenomic replicon (SGR-JFH1) cells. The viral RNA level in the cells transfected with siCKB-2 decreased by 50% compared to the control (Fig. 2A). We also tested the CKB mutant, CKB-C283S, in which Cys at aa 283, near the catalytic site, has been replaced with Ser (Fig. 3A) and which is known to be enzymatically inactive and to work in a dominant-negative manner (22, 29). As expected, overexpression of CKB-C283S resulted in a reduction in HCV RNA replication in SGR-N cells (Fig. 2B). We obtained a similar result in SGR-JFH1 cells, as described below (Fig. 3E).

To further examine the involvement of CKB in HCV RNA replication, we tested the effect of Ccr, a substrate analogue and possible inhibitor for CK in either SGR-N, SGR-JFH1 (Fig. 2C), or Huh7 cells transiently replicating luciferase-subgenomic replicon (data not shown). We found dose-dependent inhibition of HCV RNA replication but no observed effect on total cellular levels of protein and ATP (Fig. 2D) in the replicon setting used.

We next examined whether the knockdown of CKB or treatment with Ccr would abrogate the production of HCVcc. At 72 h posttransfection with siCKB-2, the HCV core level in cells infected with HCVcc was significantly reduced (Fig. 2E). Treatment of the infected cells with Ccr at various concentrations also reduced the intracellular and supernatant core level and subsequently decreased HCVcc production (Fig. 2F). These results demonstrate that suppression of the HCV RNA replication by the siRNA-mediated knockdown of CKB or treatment with CKB inhibitor leads to reduction of the production of infectious virus.

CKB interacts with HCV NS4A. Having established a role for CKB in HCV RNA replication, we then tried to determine to how CKB influences the HCV life cycle. It has been re-

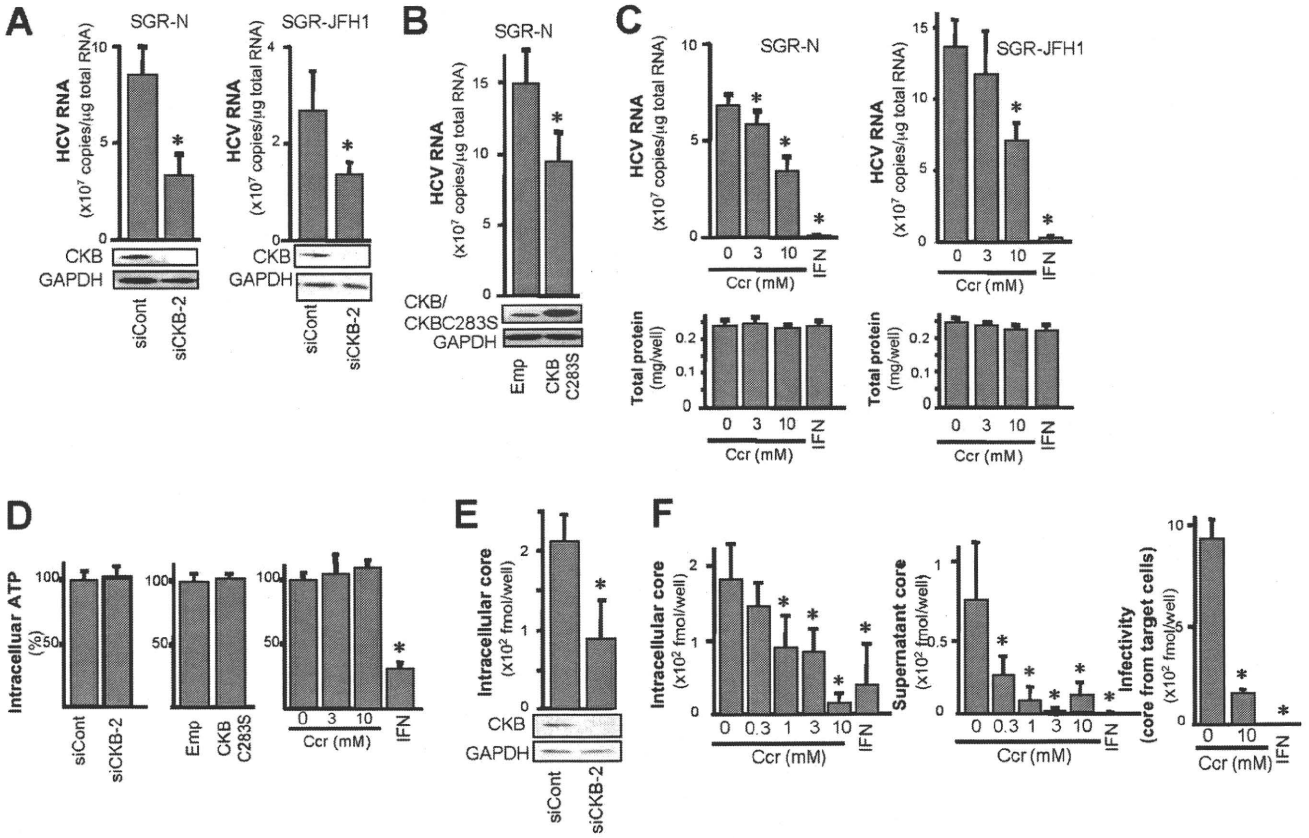

FIG. 2. Involvement of CKB in HCV replication. (A and E) Knockdown of endogenous CKB in SGR-N and SGR-JFH1 cells (A) or HCVcc-infected cells (E). Cells were transfected with siRNA against CKB (siCKB-2) or control siRNA (siCont) and were harvested at 72 h posttransfection. Real-time RT-PCR for HCV RNA levels and immunoblotting for CKB and GAPDH were performed. (B) SGR-N cells were transfected with pCAGCKB-C283S or empty vector, and HCV RNA levels and expression of CKB and CKB-C283S were determined 72 h posttransfection. SGR-N and SGR-JFH1 cells (C) or HCVcc-infected cells (F) were treated with Ccr at various concentrations for 72 h, followed by quantification of HCV RNAs and total cellular proteins. ATP levels (D) were determined after transfection with siCKB-2, pCAGCKB-C283S, or treatment with Ccr for 72 h in SGR-N cells. The ATP levels in the cells transfected with negative control siRNA (left), empty vector (middle), and no treatment (right) were set at 100%, respectively. (F) HCVcc-infected cells were treated with Ccr, and the viral core protein levels in cells (left) and supernatants (middle) were determined at 72 h postinfection. Collected culture supernatants were inoculated into naive Huh-7.5.1 cells after the removal of Ccr. After 72 h, the core proteins in cells were determined (right panel). All data are presented as averages and standard deviation values for at least triplicate samples. *, $P < 0.05$ against control such as transfection with siCont (A and E) or empty vector (B) or nontreatment (C, D, and F).

ported that interaction of CKB with some cellular proteins is required for local availability of CKB activity and local generation of ATP (22, 29). To examine the possible interaction of CKB with HCV NS proteins, HA-tagged CKB (HA-CKB) was coexpressed with FLAG-tagged NS proteins (NIHJ1 strain), followed by immunoprecipitation with an anti-FLAG antibody. CKB was shown to specifically interact with NS4A. No or little interaction was observed between CKB and either NS3, NS4B, NS5A, or NS5B (Fig. 3B). CKB-NS4A interaction was also found with the JFH-1 strain (Fig. 3C).

To identify the CKB region required for the interaction with NS4A, various deletion mutants of CKB were generated (Fig. 3A). An immunoprecipitation assay indicated that NS4A was coimmunoprecipitated with either a full-length CKB, a C-terminal deletion (aa 1 to 357), an N-terminal deletion (aa 297 to 381), or CKB-C283S, but not with aa 1 to 296, aa 1 to 247, or aa 1 to 184 (Fig. 3D, upper middle panel). Further, internal deletions of CKB (CKBdel297-357 and CKB-C283Sdel297-357) failed to interact with NS4A (Fig. 3D, lower panel), suggesting that aa 297 to 357 of CKB are important for its interaction with NS4A. It is noted that the expression of CKB aa 297 to 357 in cells was undetected, presumably due to its misfolding and/or instability. To verify a role for CKB-NS4A interaction in HCV RNA replication, we further determined the effect of expression of either CKB-C283S or its internal deletion lacking aa 297 to 357 (CKB-C283Sdel297-357) on viral replication in SGR-JFH1 cells. As expected, the HCV RNA level was significantly decreased by CKB-C283S, whereas this effect was not observed by CKB-C283Sdel297-357 (Fig. 3E).

NS4A is a 54-residue small protein composed of three domains: the N-terminal membrane anchor, the central domain responsible for interacting with NS3, and the C-terminal acidic domain. To define the portion in NS4A responsible for its interaction with CKB, we constructed three NS4A deletion mutants, each separately expressing one of the NS4A domains, with a FLAG tag (Fig. 3F). CKB proved to interact with the central domain, aa 21 to 39, of NS4A, which is involved in

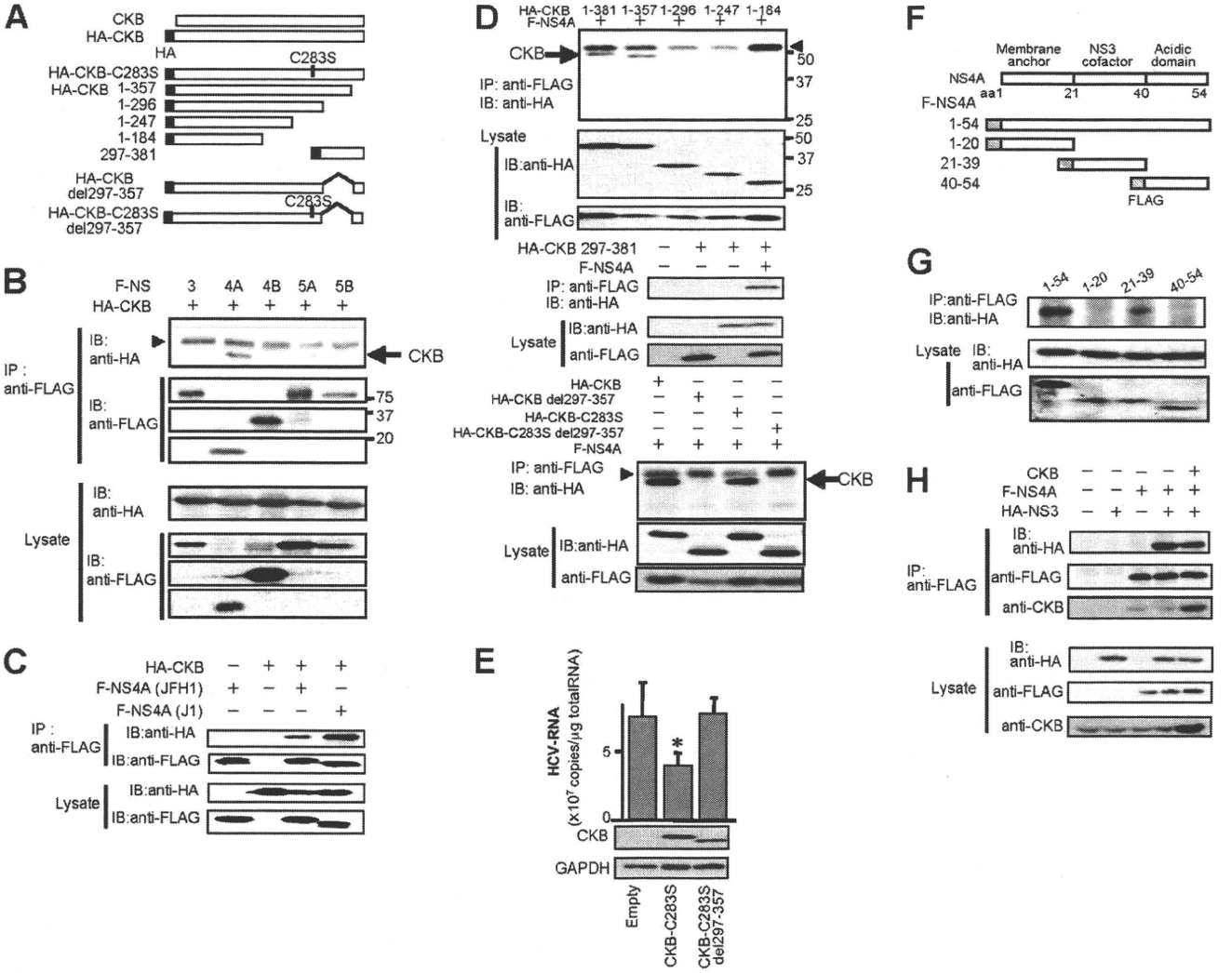

FIG. 3. CKB interacts with HCV NS4A. (A) Structures of CKB constructs used in the present study. A full-length wild-type CKB without an epitope tag (CKB) or with an N-terminal HA tag (HA-CKB), HA-CKB with deletions (aa 1 to 357, aa 1 to 296, aa 1 to 247, aa 1 to 184, and aa 297 to 381 and del297-357), CKB mutant at the catalytic site, Cys-283 (CKB-C283S) or CKB-C283S lacking aa 297 to 357 (CKB-C283Sdel297-357) are shown. HA-CKB was coexpressed with FLAG-tagged versions of each NS protein of strain NIHJ1 (B) or with NS4A of strain JFH-1 (C) in 293T cells and immunoprecipitated (IP) with an anti-FLAG antibody. Immunoprecipitates were subjected to immunoblotting (IB) with anti-HA or anti-FLAG antibody. (D) Each CKB deletion mutant was coexpressed with FLAG-NS4A in 293T cells. Immunoprecipitates were analyzed by immunoblotting. Arrow, CKB; arrowhead, immunoglobulin heavy chain. (E) SGR-JFH1 cells were transfected with the expression plasmid for CKB-C283S, CKB-C283Sdel297-357 or empty vector. At 72 h posttransfection, HCV RNA levels and the expression of CKB and CKB-C283S were determined by real-time RT-PCR and immunoblotting with anti-HA antibody, respectively. For HCV RNA quantitation, data are indicated as averages and standard deviations ($n = 3$). *, $P < 0.05$ against the empty vector control. (F) Structure of NS4A and NS4A constructs. FLAG-tagged NS4A (aa 1 to 54) or its truncated mutants (aa 1 to 20, aa 21 to 39, or aa 40 to 54) are shown. (G) Each NS4A deletion mutant was coexpressed with HA-CKB and analyzed as described above. (H) FLAG-NS4A was coexpressed with HA-NS3 or HA-NS3 and CKB, followed by immunoprecipitation with anti-FLAG antibody. Immunoprecipitates were analyzed by immunoblotting with anti-HA, anti-FLAG or anti-CKB antibody.

formation of the NS3-NS4A complex (Fig. 3G). We therefore investigate whether NS3-NS4A interaction is affected in the presence of CKB and found that exogenous expression of CKB has no influence on NS3-NS4A interaction, and a putative NS3-NS4A-CKB complex was detected in the coimmunoprecipitation analysis (Fig. 3H). Collectively, these results strongly suggest that CKB plays a key role in HCV RNA replication via interaction with NS4A.

Subcellular localization of CKB and NS4A in cells replicating HCV RNA. CKB is distributed throughout cells but is mainly localized in the perinuclear area (31), whereas NS4A is predominantly localized at the endoplasmic reticulum and mitochondrial membranes (37). We examined the possible subcellular colocalization of CKB and NS4A in SGR-N cells by immunofluorescence staining (Fig. 4A). CKB tended to gather in the perinuclear area of HCV replicating cells and was partially colocalized with NS4A in the area, sharing a dotlike structure. To further analyze the subcellular compartments in which CKB and NS4A coexist, we used double-labeling immunoelectron microscopy on SGR-N cells using antibodies against CKB and NS4A, with secondary antibodies coupled to 12- and 18-nm gold particles, respectively. One fraction of

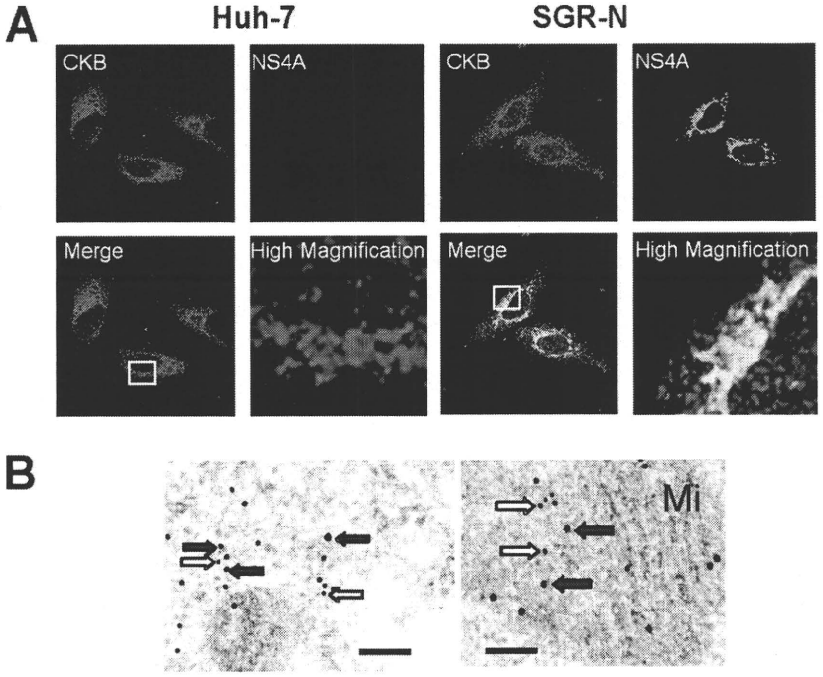

FIG. 4. Colocalization of CKB with HCV NS4A. (A) Indirect immunofluorescence analysis. The primary antibodies used were anti-CKB goat PAb (red) and anti-NS4A MAb (green). Merged images of red and green signals are shown. High-magnification panels are enlarged images of white squares in the merge panels. (B) Immunoelectron microscopic localization of CKB and NS4A. SGR-N cells were double-immunolabeled for CKB (12-nm gold particles; white arrows) and for NS4A (18-nm gold particle; gray arrows). Mi, mitochondria. Bars, 200 nm.

CKB colocalized with NS4A in the cytoplasmic electron-dense regions, presumably derived from altered or folded membrane structures (Fig. 4B, left panel) and mitochondria (Fig. 4B, right panel).

CKB enhances functional HCV replicase and NS3-4A helicase. NS4A is known to mediate membrane association of the NS3-4A complex and to function as a cofactor in NS3 enzyme activity. To understand the mechanism(s) underlying positive regulation of HCV RNA replication through CKB via its interaction with NS4A, we first investigated whether CKB modulates NS3-4A helicase activity. NS3-4A helicase is a member of the superfamily-2 DexH/D-box helicase, which unwinds RNA-RNA substrates in a 3′-to-5′ direction. During RNA replication, the NS3-4A helicase is believed to translocate along the nucleic acid substrate by changing its protein conformation, utilizing the energy of ATP hydrolysis (9). We then tested the effect of CKB on RNA- or DNA-unwinding activity using purified recombinant full-length NS3 and NS3-4A complex (12). As shown in Fig. 5A (left middle panel), both NS3 and NS3-4A helicase activity unwound dsRNA substrate most efficiently when CKB, ATP, and pCr were added to the reaction mixture. The enhancing effect of CKB was observed in the presence of pCr but not in the absence of it, suggesting that catalytic activity of CKB is important for its effect on the HCV helicase activity. Similar results were obtained from the DNA helicase assay using dsDNA substrate (Fig. 5B). To address the specificity of the stimulation by the CKB/pCr system, effects of PK and pPy, which are also involved in the ATP generation, were determined (Fig. 5A, right panels). Exogenous PK and pPy at the same concentrations as those of CKB and pCr used in the study exhibited no effect on the HCV helicase activity.

The effect of CKB on NS3-4A serine protease activity, which is considered to be ATP-independent, was also assessed in an in vitro protease assay using the purified viral proteins as mentioned above (Fig. 5C). As expected, NS3-4A complex exhibited significantly higher activity than NS3 alone; however, CKB did not affect the protease activities of NS3 or NS3-4A.

Finally, we investigated loss and gain of function of CKB in HCV replicase activity, which requires high-energy phosphate, in the context of semi-intact replicon cells. Miyanari et al. (33) reported that the function of the active HCV RC can be monitored in permeabilized replicon cells treated with digitonin. Thus, permeabilized replicon cells in the presence or absence of exogenous CKB were incubated with [α-^{32}P]UTP to detect newly synthesized RNA. As indicated in Fig. 5D, an ~8-kb band corresponding to HCV subgenomic RNA was most abundant in cells in the presence of exogenous CKB, ATP and pCr. The enhancing effect of CKB was observed in the presence but not in the absence of pCr, suggesting that catalytic activity of CKB is important for its effect on the replicase activity. As for the RNA helicase assay, exogenous PK and pPy did not enhance the replicase activity (data not shown). HCV replicase activity in permeabilized cells to which we had introduced siCKB-2 was diminished compared to that in siRNA control-treated cells. Interestingly, the replicase activity in the CKB-depleted cells was recovered by the addition of CKB. Thus, our findings suggest that CKB functions as a key regulator of HCV genome replication by controlling energy-dependent viral enzyme activities.

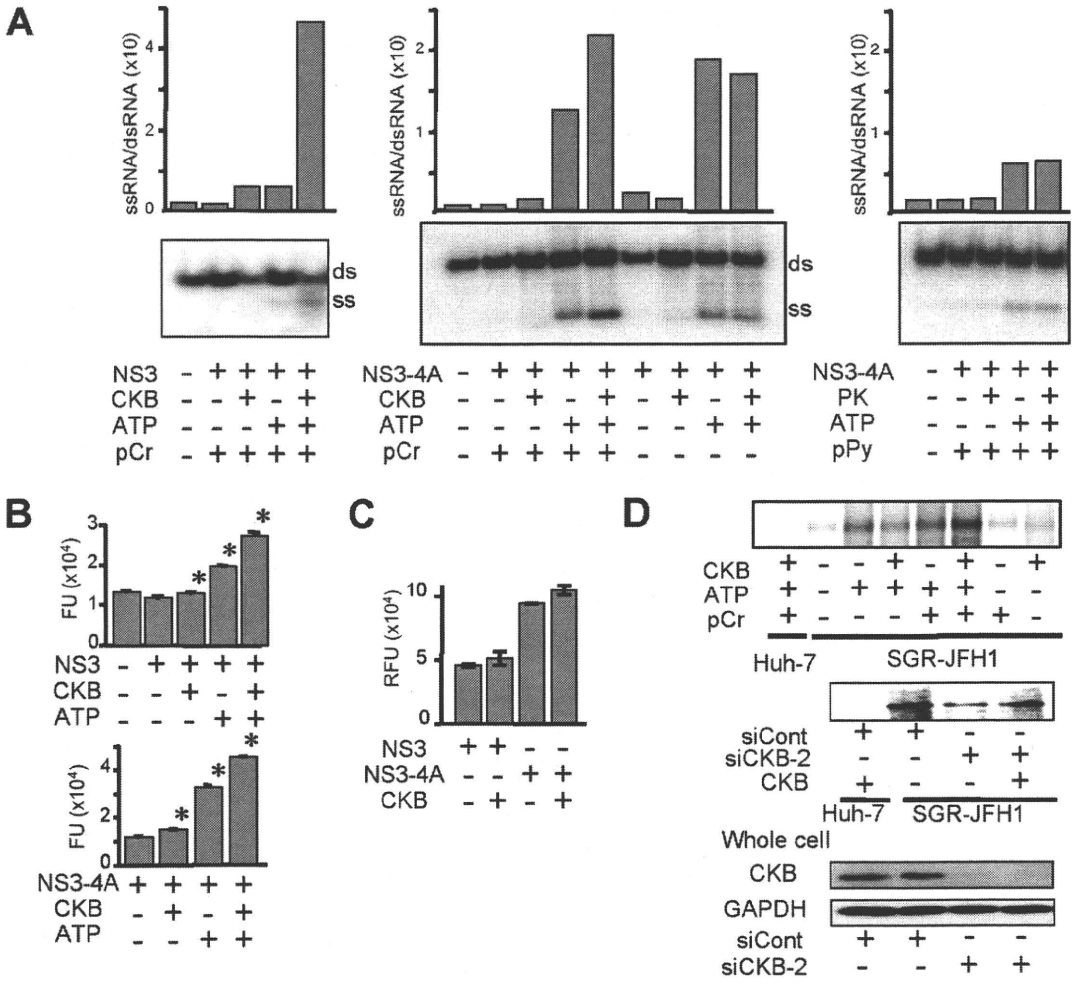

FIG. 5. CKB enhances NS3-4A helicase and HCV replicase activities. (A) In vitro RNA helicase activity of NS3-4A or NS3 was determined by detecting unwound single-strand RNA (ss) derived from the partially dsRNA substrate (ds). Band intensities corresponding to unwound products and those to dsRNA substrates were determined by ImageQuant 5.2 (Molecular Dynamics), and the ssRNA/dsRNA ratios were calculated. The results are representative of three similar experiments. (B) In vitro DNA helicase activity of NS3-4A or NS3 was analyzed by using a commercially available kit. The data represent averages and standard deviations ($n = 3$). *, $P < 0.05$ against the value without supplementation of CKB and ATP. (C) The in vitro HCV protease activity of NS3-4A or NS3 in the presence or absence of CKB was analyzed. Error bars represent standard deviations ($n = 3$). (D) Replicase activity in permeabilized replicon cells. The upper panel shows the activity for synthesis of HCV subgenomic RNA in the digitonin-permeabilized SGR-JFH1 cells with or without supplementation of CKB was measured. The middle panel shows results for SGR-JFH1 or Huh-7 cells that were transfected with siCKB-2 or siCont and permeabilized at 72 h posttransfection. The permeabilized cells with or without supplementation of CKB were subjected to the replicase assay. The lower panel shows the immunoblotting results for whole-cell lysates of siRNA-transfected cells.

DISCUSSION

Viral replication requires energy and macromolecule synthesis, and host cells provide the viruses with metabolic resources necessary for their efficient replication. Thus, it is highly likely that interaction of viruses with host cell metabolic pathways, including energy-generating systems, contributes to the virus growth cycle. In the regulation of HCV genome replication, the functions of the viral NS proteins that comprise the RC might be regulated by association in individual host cell factors. For example, hVAP-A and -B function as cofactors of modulating RC formation via interacting with NS5A and NS5B (13, 18). Cyclophilin B is involved in stimulating viral RNA binding activity via interacting with NS5B (49). FKBP8 (39) and hB-ind1 (45) play an important role in recruiting Hsp90 to RC via interacting with NS5A. However, the association of viral protein(s) with the cellular energy-generating system to directly regulate the activity of the RC has not been well understood.

In the present study, the accumulation of CKB, an ATP-generating enzyme, in the HCV RC-rich membrane fraction of viral replicating cells and its importance in replication of the HCV genome and production of infectious virions have been demonstrated. Enzymatic analyses with semi-intact replicon cells and purified NS3-4A protein revealed that CKB enhances the functional replicase and helicase of HCV. Its enhancing effect was observed in the presence of pCr but not in its absence, suggesting that the catalytic activity of CKB is important for enhancing the replicase and

helicase activities. Moreover, we clearly detected a CKB-NS4A complex using anti-tag antibodies in cotransfection experiments, but the endogenous complex could not be immunoprecipitated from cells expressing only endogenous levels of CKB, probably because of the inefficiency of the available antibodies. Further, a deletion of the NS4A-interacting region within an inactive mutant of CKB (CKB-C283S) resulted in the loss of its dominant-negative effect on HCV replication.

Creatine kinase, an evolutionarily conserved enzyme, is known to be critical for the maintenance and regulation of cellular energy stores in tissues with high and rapidly changing energy demands (48). In mammals, three cytosolic and two mitochondrial isoforms of CK, which share certain conserved regions, are expressed (35). The brain-type CK, CKB, plays a major role in cellular energy metabolism of nonmuscle cells, reversibly catalyzing the ATP-dependent phosphorylation of creatine and, hence, providing an ATP buffering system in subcellular compartments of high and fluctuating energy demand (21, 29). CKB is overexpressed in a wide range of tumor tissues and tumor cell lines, including hepatocellular carcinoma (32), and is used as a prognostic marker of cancer.

Although CK and creatine phosphate have been supplemented to in vitro replicase assays of some RNA viruses (15, 33), understanding of CKB function in the virus life cycle has been limited. One study indicated that the CK substrate analog, Ccr, exhibits antiviral activity against several herpesviruses but not influenza viruses or vesicular stomatitis virus (26). We have demonstrated here that HCV genome replication is downregulated by either treatment with Ccr, siRNA-mediated knockdown of CKB, or the exogenous expression of CKB-C283S. Coimmunoprecipitation experiments revealed that the essential domain within NS4A for the interaction with CKB is the NS4A central domain, aa 21 to 39, which is also responsible for NS3-4A complex formation. However, the NS3-4A interaction was not impaired by overexpression of CKB, and CKB was found to be able to form a complex with NS3-4A (Fig. 3H). Since CKB does not directly interact with NS3 (Fig. 3A), it is likely that NS3-4A-CKB association occurs through two interactions of NS3-4A and NS4A-CKB. We examined whether the formation of the ternary complex affects HCV enzymatic activities, possibly through conformational changes in the viral proteins, and found that CKB has no influence on NS3-4A protease activity (Fig. 5C). With regard to helicase activity, the effect of CKB on RNA unwinding activity by NS3-4A was similar to the effect of NS3 alone in the presence of ATP (Fig. 5A). It is conceivable that interaction with CKB causes no or little global change in the NS3-4A conformation and does not affect the viral helicase and protease activities.

In general, translation initiation in eukaryotes includes an ATP-dependent process such as unwinding the secondary structure in the 5′-untranslated region to permit assembly of 48S ribosomal complexes. It was reported, however, that 48S complex formation on the HCV internal ribosome entry site (IRES) has no requirement for ATP hydrolysis (25). In fact, we found that Huh-7 cells with or without gene silencing of CKB exhibited the same level of HCV IRES activity by transfection with IRES-reporter constructs (data not shown).

Collectively, we conclude that CKB is targeted to the HCV RC through its interaction with NS4A and functions as a positive regulator for the viral replicase by providing ATP. It is likely that the catalytic activity of CKB that associates with the viral RC is important for enhancing the RNA replication. The role of CKB-NS4A interaction in the enhancing effect seems to be limited. Although either knocking down CKB, expression of the dominant-negative mutant of CKB, or Ccr treatment resulted in the reduction of HCV replication (Fig. 2A to C), the total cellular ATP levels were not changed under these conditions (Fig. 2D). This suggests that CKB contributes to enhancing HCV replication through controlling the ATP level in the particular RC compartment. A tight coupling of a fast ATP regeneration and delivery system to the viral RC is advantageous for achieving efficient replication of the viral genome. To our knowledge, the findings presented here provide the first experimental evidence of the involvement of viral protein in recruiting an ATP generating/buffering system to the subcellular compartment for viral genome replication, a site with high-energy turnover. Given that the levels of HCV RNA were not dramatically diminished by the knocking down, dominant-negative mutant or Ccr, CKB may not be absolutely critical for the viral replication. One would argue that energy required for HCV genome replication can be partly complemented from the intracellular ATP pool.

Although there are several isoforms of CK as described above, the most abundant CK species expressed in Huh-7 cells in the present study was CKB, and no other isoenzymes, including mitochondrial CK, were detected by an isoform analysis based on the overlay gel technique (32; data not shown). Thus, the CKB isoenzyme appears to be a key molecule in the energy metabolism of HCV replicating cells. To identify potential HCV RC components, we used a comparative proteome analysis of the DRM fraction in cells harboring HCV subgenomic replicon and the DRM fractions in parental cells and then identified proteins that were more abundant in the fraction of HCV replicating cells. In agreement with similar previously reported approaches using the DRM or lipid raft fraction (30, 53), the functional categories of identified proteins included protein folding or assembly, cell metabolism and biosynthesis, cellular processes, and cytoskeleton organization (Table 1). Interestingly, Mannova et al. found that CKB was upregulated in the fraction of Huh-7 cells carrying the genotype 1b Con1 isolate-derived HCV replicon, as determined using stable isotope labeling by amino acids combined with one-dimensional electrophoresis (30). However, the effect of CKB on regulation of the HCV life cycle was not examined in that study.

In conclusion, CKB interacts with HCV NS4A and is important for efficient replication of the viral genome. Recruitment of CKB to the HCV replication machinery through its interaction with NS4A may have important implications for the maintenance or enhancement of the functional replicase activity in the RC compartment, where high-energy phosphoryl groups are required. A strategy for specific interception of energy supply at the subcellular site of HCV genome replication by disruption of the NS4A-CKB interface may lead to development of a new type of antiviral agent.

ACKNOWLEDGMENTS

We thank Francis V. Chisari (The Scripps Research Institute) for providing Huh-7.5.1 cells; Raffaele De Francesco (Istituto di Ricerche

di Biologia Molecolare, P. Angeletti) for providing purified recombinant NS3 and NS3-4A proteins; Oriental Yeast Co., Ltd., for providing human CKB cDNA; Minoru Fukuda (Laboratory for Electron Microscopy, Kyorin University School of Medicine) for electron microscopy; S. Yoshizaki, T. Shimoji, M. Kaga, M. Sasaki, and T. Date for technical assistance; and T. Mizoguchi for secretarial work.

This study was supported by a grant-in-aid for Scientific Research from the Japan Society for the Promotion of Science, from the Ministry of Health, Labor, and Welfare of Japan and from the Ministry of Education, Culture, Sports, Science, and Technology and by Research on Health Sciences focusing on Drug Innovation from the Japan Health Sciences Foundation, Japan, and by the Program for Promotion of Fundamental Studies in Health Sciences of the National Institute of Biomedical Innovation of Japan.

REFERENCES

1. **Aizaki, H., Y. Aoki, T. Harada, K. Ishii, T. Suzuki, S. Nagamori, G. Toda, Y. Matsuura, and T. Miyamura.** 1998. Full-length complementary DNA of hepatitis C virus genome from an infectious blood sample. Hepatology **27:** 621–627.
2. **Aizaki, H., K. J. Lee, V. M. Sung, H. Ishiko, and M. M. Lai.** 2004. Characterization of the hepatitis C virus RNA replication complex associated with lipid rafts. Virology **324:**450–461.
3. **Aizaki, H., K. Morikawa, M. Fukasawa, H. Hara, Y. Inoue, H. Tani, K. Saito, M. Nishijima, K. Hanada, Y. Matsuura, M. M. Lai, T. Miyamura, T. Wakita, and T. Suzuki.** 2008. Critical role of virion-associated cholesterol and sphingolipid in hepatitis C virus infection. J. Virol. **82:**5715–5724.
4. **Alter, H. J., and L. B. Seeff.** 2000. Recovery, persistence, and sequelae in hepatitis C virus infection: a perspective on long-term outcome. Semin. Liver Dis. **20:**17–35.
5. **Aoyagi, K., C. Ohue, K. Iida, T. Kimura, E. Tanaka, K. Kiyosawa, and S. Yagi.** 1999. Development of a simple and highly sensitive enzyme immunoassay for hepatitis C virus core antigen. J. Clin. Microbiol. **37:**1802–1808.
6. **Appel, N., T. Schaller, F. Penin, and R. Bartenschlager.** 2006. From structure to function: new insights into hepatitis C virus RNA replication. J. Biol. Chem. **281:**9833–9836.
7. **Bartenschlager, R., and V. Lohmann.** 2001. Novel cell culture systems for the hepatitis C virus. Antivir. Res. **52:**1–17.
8. **Brass, V., J. M. Berke, R. Montserret, H. E. Blum, F. Penin, and D. Moradpour.** 2008. Structural determinants for membrane association and dynamic organization of the hepatitis C virus NS3-4A complex. Proc. Natl. Acad. Sci. USA.
9. **Dumont, S., W. Cheng, V. Serebrov, R. K. Beran, I. Tinoco, Jr., A. M. Pyle, and C. Bustamante.** 2006. RNA translocation and unwinding mechanism of HCV NS3 helicase and its coordination by ATP. Nature **439:**105–108.
10. **Failla, C., L. Tomei, and R. De Francesco.** 1994. Both NS3 and NS4A are required for proteolytic processing of hepatitis C virus nonstructural proteins. J. Virol. **68:**3753–3760.
11. **Gallinari, P., D. Brennan, C. Nardi, M. Brunetti, L. Tomei, C. Steinkuhler, and R. De Francesco.** 1998. Multiple enzymatic activities associated with recombinant NS3 protein of hepatitis C virus. J. Virol. **72:**6758–6769.
12. **Gallinari, P., C. Paolini, D. Brennan, C. Nardi, C. Steinkuhler, and R. De Francesco.** 1999. Modulation of hepatitis C virus NS3 protease and helicase activities through the interaction with NS4A. Biochemistry **38:**5620–5632.
13. **Gao, L., H. Aizaki, J. W. He, and M. M. Lai.** 2004. Interactions between viral nonstructural proteins and host protein hVAP-33 mediate the formation of hepatitis C virus RNA replication complex on lipid raft. J. Virol. **78:**3480–3488.
14. **Gosert, R., D. Egger, V. Lohmann, R. Bartenschlager, H. E. Blum, K. Bienz, and D. Moradpour.** 2003. Identification of the hepatitis C virus RNA replication complex in Huh-7 cells harboring subgenomic replicons. J. Virol. **77:**5487–5492.
15. **Green, K. Y., A. Mory, M. H. Fogg, A. Weisberg, G. Belliot, M. Wagner, T. Mitra, E. Ehrenfeld, C. E. Cameron, and S. V. Sosnovtsev.** 2002. Isolation of enzymatically active replication complexes from feline calicivirus-infected cells. J. Virol. **76:**8582–8595.
16. **Guidotti, L. G., and F. V. Chisari.** 2006. Immunobiology and pathogenesis of viral hepatitis. Annu. Rev. Pathol. **1:**23–61.
17. **Guo, J. T., V. V. Bichko, and C. Seeger.** 2001. Effect of alpha interferon on the hepatitis C virus replicon. J. Virol. **75:**8516–8523.
18. **Hamamoto, I., Y. Nishimura, T. Okamoto, H. Aizaki, M. Liu, Y. Mori, T. Abe, T. Suzuki, M. M. Lai, T. Miyamura, K. Moriishi, and Y. Matsuura.** 2005. Human VAP-B is involved in hepatitis C virus replication through interaction with NS5A and NS5B. J. Virol. **79:**13473–13482.
19. **Hoofnagle, J. H.** 2002. Course and outcome of hepatitis C. Hepatology **36:**S21–S29.
20. **Ichimura, T., H. Yamamura, K. Sasamoto, Y. Tominaga, M. Taoka, K. Kakiuchi, T. Shinkawa, N. Takahashi, S. Shimada, and T. Isobe.** 2005. 14-3-3 proteins modulate the expression of epithelial Na+ channels by phosphorylation-dependent interaction with Nedd4-2 ubiquitin ligase. J. Biol. Chem. **280:**13187–13194.
21. **Inoue, K., S. Ueno, and A. Fukuda.** 2004. Interaction of neuron-specific K^+-Cl^- cotransporter, KCC2, with brain-type creatine kinase. FEBS Lett. **564:**131–135.
22. **Inoue, K., J. Yamada, S. Ueno, and A. Fukuda.** 2006. Brain-type creatine kinase activates neuron-specific K^+-Cl^- cotransporter KCC2. J. Neurochem. **96:**598–608.
23. **Kato, T., T. Date, M. Miyamoto, A. Furusaka, K. Tokushige, M. Mizokami, and T. Wakita.** 2003. Efficient replication of the genotype 2a hepatitis C virus subgenomic replicon. Gastroenterology **125:**1808–1817.
24. **Kato, T., A. Furusaka, M. Miyamoto, T. Date, K. Yasui, J. Hiramoto, K. Nagayama, T. Tanaka, and T. Wakita.** 2001. Sequence analysis of hepatitis C virus isolated from a fulminant hepatitis patient. J. Med. Virol. **64:**334–339.
25. **Lancaster, A. M., E. Jan, and P. Sarnow.** 2006. Initiation factor-independent translation mediated by the hepatitis C virus internal ribosome entry site. RNA **12:**894–902.
26. **Lillie, J. W., D. F. Smee, J. H. Huffman, L. J. Hansen, R. W. Sidwell, and R. Kaddurah-Daouk.** 1994. Cyclocreatine (1-carboxymethyl-2-iminoimidazolidine) inhibits the replication of human herpesviruses. Antivir. Res. **23:**203–218.
27. **Lindenbach, B. D., M. J. Evans, A. J. Syder, B. Wolk, T. L. Tellinghuisen, C. C. Liu, T. Maruyama, R. O. Hynes, D. R. Burton, J. A. McKeating, and C. M. Rice.** 2005. Complete replication of hepatitis C virus in cell culture. Science **309:**623–626.
28. **Lindenbach, B. D., B. M. Pragai, R. Montserret, R. K. Beran, A. M. Pyle, F. Penin, and C. M. Rice.** 2007. The C terminus of hepatitis C virus NS4A encodes an electrostatic switch that regulates NS5A hyperphosphorylation and viral replication. J. Virol. **81:**8905–8918.
29. **Mahajan, V. B., K. S. Pai, A. Lau, and D. D. Cunningham.** 2000. Creatine kinase, an ATP-generating enzyme, is required for thrombin receptor signaling to the cytoskeleton. Proc. Natl. Acad. Sci. USA **97:**12062–12067.
30. **Mannova, P., R. Fang, H. Wang, B. Deng, M. W. McIntosh, S. M. Hanash, and L. Beretta.** 2006. Modification of host lipid raft proteome upon hepatitis C virus replication. Mol. Cell Proteomics **5:**2319–2325.
31. **Manos, P., and J. Edmond.** 1992. Immunofluorescent analysis of creatine kinase in cultured astrocytes by conventional and confocal microscopy: a nuclear localization. J. Comp. Neurol. **326:**273–282.
32. **Meffert, G., F. N. Gellerich, R. Margreiter, and M. Wyss.** 2005. Elevated creatine kinase activity in primary hepatocellular carcinoma. BMC Gastroenterol. **5:**9.
33. **Miyanari, Y., M. Hijikata, M. Yamaji, M. Hosaka, H. Takahashi, and K. Shimotohno.** 2003. Hepatitis C virus nonstructural proteins in the probable membranous compartment function in viral genome replication. J. Biol. Chem. **278:**50301–50308.
34. **Moradpour, D., F. Penin, and C. M. Rice.** 2007. Replication of hepatitis C virus. Nat. Rev. Microbiol. **5:**453–463.
35. **Muhlebach, S. M., M. Gross, T. Wirz, T. Wallimann, J. C. Perriard, and M. Wyss.** 1994. Sequence homology and structure predictions of the creatine kinase isoenzymes. Mol. Cell Biochem. **133–134:**245–262.
36. **Murakami, K., K. Ishii, Y. Ishihara, S. Yoshizaki, K. Tanaka, Y. Gotoh, H. Aizaki, M. Kohara, H. Yoshioka, Y. Mori, N. Manabe, I. Shoji, T. Sata, R. Bartenschlager, Y. Matsuura, T. Miyamura, and T. Suzuki.** 2006. Production of infectious hepatitis C virus particles in three-dimensional cultures of the cell line carrying the genome-length dicistronic viral RNA of genotype 1b. Virology **351:**381–392.
37. **Nomura-Takigawa, Y., M. Nagano-Fujii, L. Deng, S. Kitazawa, S. Ishido, K. Sada, and H. Hotta.** 2006. Non-structural protein 4A of Hepatitis C virus accumulates on mitochondria and renders the cells prone to undergoing mitochondria-mediated apoptosis. J. Gen. Virol. **87:**1935–1945.
38. **Ohara-Imaizumi, M., T. Fujiwara, Y. Nakamichi, T. Okamura, Y. Akimoto, J. Kawai, S. Matsushima, H. Kawakami, T. Watanabe, K. Akagawa, and S. Nagamatsu.** 2007. Imaging analysis reveals mechanistic differences between first- and second-phase insulin exocytosis. J. Cell Biol. **177:**695–705.
39. **Okamoto, T., Y. Nishimura, T. Ichimura, K. Suzuki, T. Miyamura, T. Suzuki, K. Moriishi, and Y. Matsuura.** 2006. Hepatitis C virus RNA replication is regulated by FKBP8 and Hsp90. EMBO J. **25:**5015–5025.
40. **Oliver, I. T.** 1955. A spectrophotometric method for the determination of creatine phosphokinase and myokinase. Biochem. J. **61:**116–122.
41. **Shi, S. T., K. J. Lee, H. Aizaki, S. B. Hwang, and M. M. Lai.** 2003. Hepatitis C virus RNA replication occurs on a detergent-resistant membrane that cofractionates with caveolin-2. J. Virol. **77:**4160–4168.
42. **Shirakura, M., K. Murakami, T. Ichimura, R. Suzuki, T. Shimoji, K. Fukuda, K. Abe, S. Sato, M. Fukasawa, Y. Yamakawa, M. Nishijima, K. Moriishi, Y. Matsuura, T. Wakita, T. Suzuki, P. M. Howley, T. Miyamura, and I. Shoji.** 2007. E6AP ubiquitin ligase mediates ubiquitylation and degradation of hepatitis C virus core protein. J. Virol. **81:**1174–1185.
43. **Sunahara, Y., K. Uchida, T. Tanaka, H. Matsukawa, M. Inagaki, and Y. Matuo.** 2001. Production of recombinant human creatine kinase (r-hCK) isozymes by tandem repeat expression of M and B genes and characterization of r-hCK-MB. Clin. Chem. **47:**471–476.

44. **Suzuki, T., K. Ishii, H. Aizaki, and T. Wakita.** 2007. Hepatitis C viral life cycle. Adv. Drug Deliv. Rev. **59:**1200–1212.
45. **Taguwa, S., T. Okamoto, T. Abe, Y. Mori, T. Suzuki, K. Moriishi, and Y. Matsuura.** 2008. Human butyrate-induced transcript 1 interacts with hepatitis C virus NS5A and regulates viral replication. J. Virol. **82:**2631–2641.
46. **Takeuchi, T., A. Katsume, T. Tanaka, A. Abe, K. Inoue, K. Tsukiyama-Kohara, R. Kawaguchi, S. Tanaka, and M. Kohara.** 1999. Real-time detection system for quantification of hepatitis C virus genome. Gastroenterology **116:**636–642.
47. **Wakita, T., T. Pietschmann, T. Kato, T. Date, M. Miyamoto, Z. Zhao, K. Murthy, A. Habermann, H. G. Krausslich, M. Mizokami, R. Bartenschlager, and T. J. Liang.** 2005. Production of infectious hepatitis C virus in tissue culture from a cloned viral genome. Nat. Med. **11:**791–796.
48. **Wallimann, T., M. Wyss, D. Brdiczka, K. Nicolay, and H. M. Eppenberger.** 1992. Intracellular compartmentation, structure and function of creatine kinase isoenzymes in tissues with high and fluctuating energy demands: the 'phosphocreatine circuit' for cellular energy homeostasis. Biochem. J. **281**(Pt. 1):21–40.
49. **Watashi, K., N. Ishii, M. Hijikata, D. Inoue, T. Murata, Y. Miyanari, and K. Shimotohno.** 2005. Cyclophilin B is a functional regulator of hepatitis C virus RNA polymerase. Mol. Cell **19:**111–122.
50. **Wolk, B., D. Sansonno, H. G. Krausslich, F. Dammacco, C. M. Rice, H. E. Blum, and D. Moradpour.** 2000. Subcellular localization, stability, and trans-cleavage competence of the hepatitis C virus NS3-NS4A complex expressed in tetracycline-regulated cell lines. J. Virol. **74:**2293–2304.
51. **Wyss, M., and R. Kaddurah-Daouk.** 2000. Creatine and creatinine metabolism. Physiol. Rev. **80:**1107–1213.
52. **Yi, M., R. A. Villanueva, D. L. Thomas, T. Wakita, and S. M. Lemon.** 2006. Production of infectious genotype 1a hepatitis C virus (Hutchinson strain) in cultured human hepatoma cells. Proc. Natl. Acad. Sci. USA **103:**2310–2315.
53. **Yi, Z., C. Fang, T. Pan, J. Wang, P. Yang, and Z. Yuan.** 2006. Subproteomic study of hepatitis C virus replicon reveals Ras-GTPase-activating protein binding protein 1 as potential HCV RC component. Biochem. Biophys. Res. Commun. **350:**174–178.
54. **Zhong, J., P. Gastaminza, G. Cheng, S. Kapadia, T. Kato, D. R. Burton, S. F. Wieland, S. L. Uprichard, T. Wakita, and F. V. Chisari.** 2005. Robust hepatitis C virus infection in vitro. Proc. Natl. Acad. Sci. USA **102:**9294–9299.

JOURNAL OF VIROLOGY, Mar. 2009, p. 2389–2392 Vol. 83, No. 5
0022-538X/09/$08.00+0 doi:10.1128/JVI.01690-08

Proteasomal Turnover of Hepatitis C Virus Core Protein Is Regulated by Two Distinct Mechanisms: a Ubiquitin-Dependent Mechanism and a Ubiquitin-Independent but PA28γ-Dependent Mechanism▽

Ryosuke Suzuki,[1] Kohji Moriishi,[2] Kouichirou Fukuda,[1] Masayuki Shirakura,[1] Koji Ishii,[1] Ikuo Shoji,[3] Takaji Wakita,[1] Tatsuo Miyamura,[1] Yoshiharu Matsuura,[2] and Tetsuro Suzuki[1]*

Department of Virology II, National Institute of Infectious Diseases, Tokyo 162-8640,[1] Department of Molecular Virology, Research Institute for Microbial Diseases, Osaka University, Osaka 565-0871,[2] and Division of Microbiology, Kobe University Graduate School of Medicine, Hyogo 650-0017,[3] Japan

Received 8 August 2008/Accepted 5 December 2008

We have previously reported on the ubiquitylation and degradation of hepatitis C virus core protein. Here we demonstrate that proteasomal degradation of the core protein is mediated by two distinct mechanisms. One leads to polyubiquitylation, in which lysine residues in the N-terminal region are preferential ubiquitylation sites. The other is independent of the presence of ubiquitin. Gain- and loss-of-function analyses using lysineless mutants substantiate the hypothesis that the proteasome activator PA28γ, a binding partner of the core, is involved in the ubiquitin-independent degradation of the core protein. Our results suggest that turnover of this multifunctional viral protein can be tightly controlled via dual ubiquitin-dependent and -independent proteasomal pathways.

Hepatitis C virus (HCV) core protein, whose amino acid sequence is highly conserved among different HCV strains, not only is involved in the formation of the HCV virion but also has a number of regulatory functions, including modulation of signaling pathways, cellular and viral gene expression, cell transformation, apoptosis, and lipid metabolism (reviewed in references 9 and 15). We have previously reported that the E6AP E3 ubiquitin (Ub) ligase binds to the core protein and plays an important role in polyubiquitylation and proteasomal degradation of the core protein (22). Another study from our group identified the proteasome activator PA28γ/REG-γ as an HCV core-binding partner, demonstrating degradation of the core protein via a PA28γ-dependent pathway (16, 17). In this work, we further investigated the molecular mechanisms underlying proteasomal degradation of the core protein and found that in addition to regulation by the Ub-mediated pathway, the turnover of the core protein is also regulated by PA28γ in a Ub-independent manner.

Although ubiquitylation of substrates generally requires at least one Lys residue to serve as a Ub acceptor site (5), there is no consensus as to the specificity of the Lys targeted by Ub (4, 8). To determine the sites of Ub conjugation in the core protein, we used site-directed mutagenesis to replace individual Lys residues or clusters of Lys residues with Arg residues in the N-terminal 152 amino acids (aa) of the core (C152), within which is contained all seven Lys residues (Fig. 1A). Plasmids expressing a variety of mutated core proteins were generated by PCR and inserted into the pCAGGS (18). Each core-expressing construct was transfected into human embryonic kidney 293T cells along with the pMT107 (25) encoding a Ub moiety tagged with six His residues (His_6). Transfected cells were treated with the proteasome inhibitor MG132 for 14 h to maximize the level of Ub-conjugated core intermediates by blocking the proteasome pathway and were harvested 48 h posttransfection. His_6-tagged proteins were purified from the extracts by Ni^{2+}-chelation chromatography. Eluted protein and whole lysates of transfected cells before purification were analyzed by Western blotting using anticore antibodies (Fig. 1B). Mutations replacing one or two Lys residues with Arg in the core protein did not affect the efficiency of ubiquitylation: detection of multiple Ub-conjugated core intermediates was observed in the mutant core proteins comparable to the results seen with the wild-type core protein as previously reported (23). In contrast, a substitution of four N-terminal Lys residues (C152K6-23R) caused a significant reduction in ubiquitylation (Fig. 1B, lane 9). Multiple Ub-conjugated core intermediates were not detected in the Lys-less mutant (C152KR), in which all seven Lys residues were replaced with Arg (Fig. 1B, lane 11). These results suggest that there is not a particular Lys residue in the core protein to act as the Ub acceptor but that more than one Lys located in its N-terminal region can serve as the preferential ubiquitylation site. In rare cases, Ub is known to be conjugated to the N terminus of proteins; however, these results indicate that this does not occur within the core protein.

To investigate how polyubiquitylation correlates with proteasome degradation of the core protein, we performed kinetic analysis of the wild-type and mutated core proteins by use of the Ub protein reference (UPR) technique, which can compensate for data scatter of sample-to-sample variations such as levels of expression (10, 24). Fusion proteins expressed from UPR-based constructs (Fig. 2A) were cotranslationally cleaved by deubiquitylating enzymes, thereby generating equimolar quantities of the core proteins and the reference protein, dihydrofolate reductase-hemagglutinin (DHFR-HA) tag-modified Ub, in which the Lys at aa 48 was replaced by Arg to prevent its polyubiquitylation (Ub^{R48}). After 24 h of transfec-

* Corresponding author. Mailing address: Department of Virology II, National Institute of Infectious Diseases, 1-23-1 Toyama, Shinjuku-ku, Tokyo 162-8640, Japan. Phone: 81-3-5285-1111. Fax: 81-3-5285-1161. E-mail: tesuzuki@nih.go.jp.

▽ Published ahead of print on 17 December 2008.

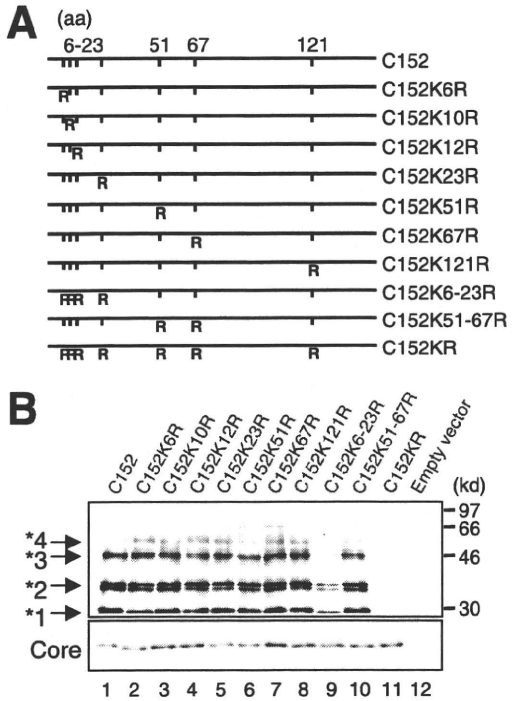

FIG. 1. In vivo ubiquitylation of HCV core protein. (A) The HCV core protein (N-terminal 152 aa) is represented on the top. The positions of the amino acid residues of the core protein are indicated above the bold lines. The positions of the seven Lys residues in the core are marked by vertical ticks. Substitution of Lys with Arg (R) is schematically depicted. (B) Detection of ubiquitylated forms of the core proteins. The transfected cells with core expression plasmids and pMT107 were treated with the proteasome inhibitor MG132 and harvested 48 h after transfection. His_6-tagged proteins were purified and subsequently analyzed by Western blot analysis using anticore antibody (upper panel). Core proteins conjugated to a number of His_6-Ub are denoted with asterisks. Whole lysates of transfected cells before purification were also analyzed (lower panel). Lanes 1 to 11, C152 to C152KR, as indicated for panel A. Lane 12; empty vector.

tion with UPR constructs, cells were treated with cycloheximide and the amounts of core proteins and DHFR-HA-Ub^{R48} at the indicated time points were determined by Western blot analysis using anticore and anti-HA antibodies. The mature form of the core protein, aa 1 to 173 (C173) (13, 20), and C152 were degraded with first-order kinetics (Fig. 2B and D). MG132 completely blocked the degradation of C173 and C152 (Fig. 2B), and C152K6-23R and C152KR were markedly stabilized (Fig. 2C). The half-lives of C173 and C152 were calculated to be 5 to 6 h, whereas those of C152K6-23R and C152KR were calculated to be 22 to 24 h (Fig. 2D), confirming that the Ub plays an important role in regulating degradation of the core protein. Nevertheless, these results also suggest possible involvement of the Ub-independent pathway in the turnover of the core protein, as C152KR is more destabilized than the reference protein (Fig. 2C and 2D).

We have shown that PA28γ specifically binds to the core protein and is involved in its degradation (16, 17). Recent studies demonstrated that PA28γ is responsible for Ub-independent degradation of the steroid receptor coactivator SRC-3 and cell cycle inhibitors such as p21 (3, 11, 12). Thus, we next investigated the possibility of PA28γ involvement in the deg-

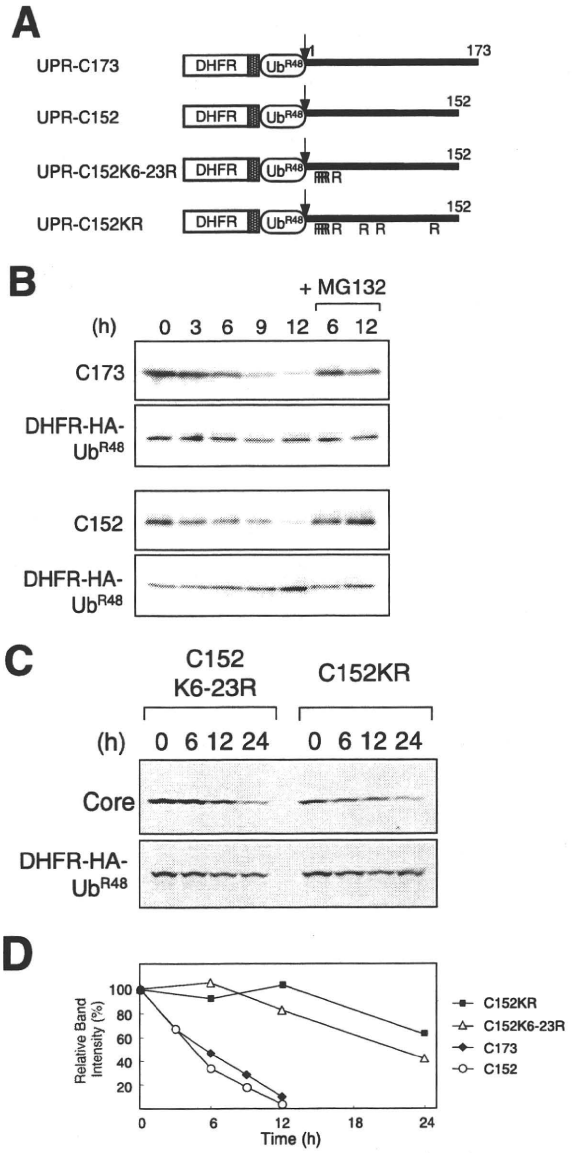

FIG. 2. Kinetic analysis of degradation of HCV core proteins. (A) The fusion constructs used in the UPR technique. Open boxes indicate the DHFR sequence, which is extended at the C terminus by a sequence containing the HA epitope (hatched boxes). Ub^{R48} moieties bearing the Lys-Arg substitution at aa 48 are represented by open ellipses. Bold lines indicate the regions of the core protein. The amino acid positions of the core protein are indicated above the bold lines. The arrows indicate the sites of in vivo cleavage by deubiquitylating enzymes. (B and C) Turnover of the core proteins. After a 24-h transfection with each UPR construct, cells were treated with 50 μg of cycloheximide/ml in the presence or absence of 10 μM MG132 for the different time periods indicated. Cells were lysed at the different time points indicated, followed by evaluation via sodium dodecyl sulfate-polyacrylamide gel electrophoresis and Western blot analysis using antibodies against the core protein and HA. (D) Quantitation of the data shown in panels B and C. At each time point, the ratio of band intensity of the core protein relative to the reference DHFR-HA-Ub^{R48} was determined by densitometry and is plotted as a percentage of the ratio at time zero.

radation of either C152KR or C152. Since C152KR carries two amino acid substitutions in the PA28γ-binding region (aa 44 to 71) (17), we tested the influence of the mutations of C152KR on the interaction with PA28γ by use of a coimmunoprecipi-

tation assay. When Flag-tagged PA28γ (F-PA28γ) was expressed in cells along with C152 or C152KR, F-PA28γ precipitated along with both C152 and C152KR, indicating that PA28γ interacts with both core proteins (Fig. 3A). Figure 3B reveals the effect of exogenous expression of F-PA28γ on the steady-state levels of C152 and C152KR. Consistent with previous data (17), the expression level of C152 was decreased to a nearly undetectable level in the presence of PA28γ (Fig. 3B, lanes 1 and 3). Interestingly, exogenous expression of PA28γ led to a marked reduction in the amount of C152KR expressed (Fig. 3B, lanes 5 and 7). Treatment with MG132 increased the steady-state level of the C152KR in the presence of F-PA28γ as well as the level of C152 (Fig. 3B, lanes 4 and 8).

We further investigated whether PA28γ affects the turnover of Lys-less core protein through time course experiments. C152KR was rapidly destabilized and almost completely degraded in a 3-h chase experiment using cells overexpressing F-PA28γ (Fig. 3C, left panels). A similar result was obtained using an analogous Lys-less mutant of the full-length core protein C191KR (Fig. 3C, right panels), thus demonstrating that the Lys-less core protein undergoes proteasomal degradation in a PA28γ-dependent manner. These results suggest that PA28γ may play a role in accelerating the turnover of the HCV core protein that is independent of ubiquitylation.

Finally, we examined gain- and loss-of-function of PA28γ with respect to degradation of full-length wild-type (C191) and mutated (C191KR) core proteins in human hepatoma Huh-7 cells. As expected, exogenous expression of PA28γ or E6AP caused a decrease in the C191 steady-state levels (Fig. 4A). In contrast, the C191KR level was decreased with expression of PA28γ but not of E6AP. We further used RNA interference to inhibit expression of PA28γ or E6AP. An increase in the abundance of C191KR was observed with PA28γ small interfering RNA (siRNA) but not with E6AP siRNA (Fig. 4B). An increase in the C191 level caused by the activity of siRNA against PA28γ or E6AP was confirmed as well.

Taking these results together, we conclude that turnover of the core protein is regulated by both Ub-dependent and Ub-independent pathways and that PA28γ is possibly involved in Ub-independent proteasomal degradation of the core protein. PA28 is known to specifically bind and activate the 20S proteasome (19). Thus, PA28γ may function by facilitating the delivery of the core protein to the proteasome in a Ub-independent manner.

Accumulating evidence suggests the existence of proteasome-dependent but Ub-independent pathways for protein degradation, and several important molecules, such as p53, p73, Rb, SRC-3, and the hepatitis B virus X protein, have two distinct degradation pathways that function in a Ub-dependent and Ub-independent manner (1, 2, 6, 7, 14, 21, 27). Recently, critical roles for PA28γ in the Ub-independent pathway have been demonstrated; SRC-3 and p21 can be recognized by the 20S proteasome independently of ubiquitylation through their interaction with PA28γ (3, 11, 12). It has also been reported that phosphorylation-dependent ubiquitylation mediated by GSK3 and SCF is important for SRC-3 turnover (26). Nevertheless, the precise mechanisms underlying turnover of most of the proteasome substrates that are regulated in both Ub-dependent and Ub-independent manners are not well understood. To our knowledge, the HCV core protein is the first

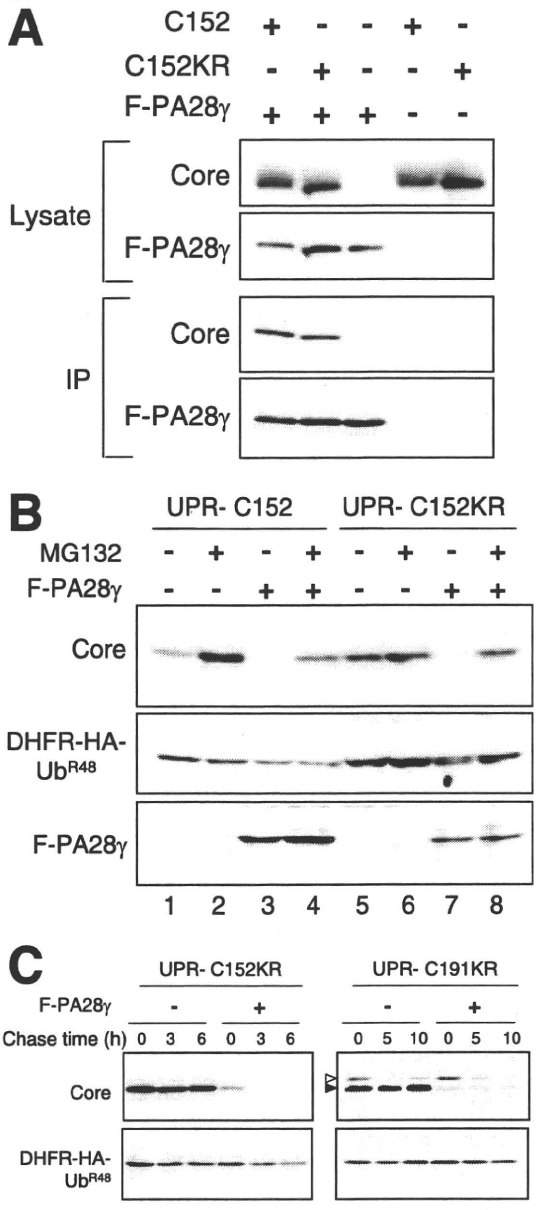

FIG. 3. PA28γ-dependent degradation of the core protein. (A) Interaction of the core protein with PA28γ. Cells were cotransfected with the wild-type (C152) or Lys-less (C152KR) core expression plasmid in the presence of a Flag-PA28γ (F-PA28γ) expression plasmid or an empty vector. The transfected cells were treated with MG132. After 48 h, the cell lysates were immunoprecipitated with anti-Flag antibody and visualized by Western blotting with anticore antibodies. Western blot analysis of whole cell lysates was also performed. (B) Degradation of the wild-type and Lys-less core proteins via the PA28γ-dependent pathway. Cells were transfected with the UPR construct with or without F-PA28γ. In some cases, cells were treated with 10 μM MG132 for 14 h before harvesting. Western blot analysis was performed using anticore, anti-HA, and anti-Flag antibodies. (C) After 24 h of transfection with UPR-C152KR and UPR-C191KR with or without F-PA28γ (an empty vector), cells were treated with 50 μg of cycloheximide/ml for different time periods as indicated (chase time). Western blot analysis was performed using anticore and anti-HA antibodies. The precursor core protein and the core that was processed, presumably by signal peptide peptidase, are denoted by open and closed triangles, respectively.

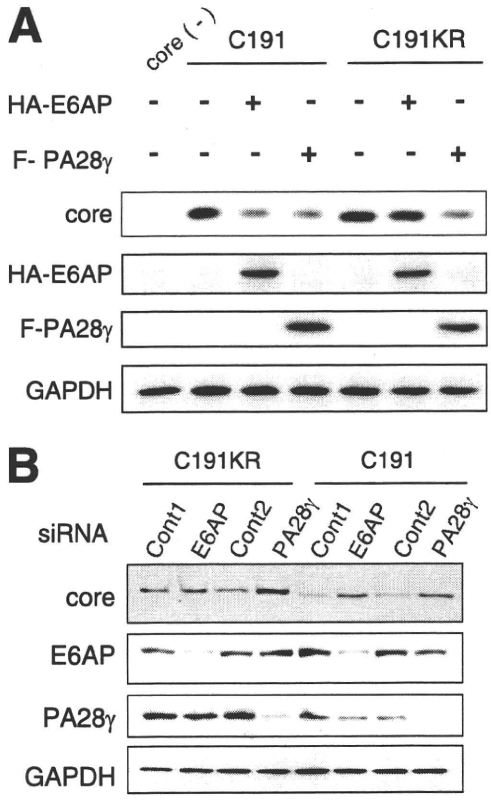

FIG. 4. Ub-dependent and Ub-independent degradation of the full-length core protein in hepatic cells. (A) Huh-7 cells were cotransfected with plasmids for the full-length core protein (C191) or its Lys-less mutant (C191KR) in the presence of F-PA28γ or HA-tagged-E6AP expression plasmid (HA-E6AP). After 48 h, cells were lysed and Western blot analysis was performed using anticore, anti-HA, anti-Flag, or anti-GAPDH. (B) Huh-7 cells were cotransfected with core expression plasmids along with siRNA against PA28γ or E6AP or with negative control siRNA. Cells were harvested 72 h after transfection and subjected to Western blot analysis.

viral protein studied that has led to identification of key cellular factors responsible for proteasomal degradation via dual distinct mechanisms. Although the question remains whether there is a physiological significance of the Ub-dependent and Ub-independent degradation of the core protein, it is reasonable to consider that tight control over cellular levels of the core protein, which is multifunctional and essential for viral replication, maturation, and pathogenesis, may play an important role in representing the potential for its functional activity.

This work was supported by a grant-in-aid for Scientific Research from the Japan Society for the Promotion of Science, from the Ministry of Health, Labor and Welfare of Japan, and from the Ministry of Education, Culture, Sports, Science and Technology, by Research on Health Sciences focusing on Drug Innovation from the Japan Health Sciences Foundation, Japan, and by the Program for Promotion of Fundamental Studies in Health Sciences of the National Institute of Biomedical Innovation of Japan.

REFERENCES

1. **Asher, G., J. Lotem, L. Sachs, C. Kahana, and Y. Shaul.** 2002. Mdm-2 and ubiquitin-independent p53 proteasomal degradation regulated by NQO1. Proc. Natl. Acad. Sci. USA **99:**13125–13130.
2. **Asher, G., P. Tsvetkov, C. Kahana, and Y. Shaul.** 2005. A mechanism of ubiquitin-independent proteasomal degradation of the tumor suppressors p53 and p73. Genes Dev. **19:**316–321.
3. **Chen, X., L. F. Barton, Y. Chi, B. E. Clurman, and J. M. Roberts.** 2007. Ubiquitin-independent degradation of cell-cycle inhibitors by the REGγ proteasome. Mol. Cell **26:**843–852.
4. **Ciechanover, A.** 1998. The ubiquitin-proteasome pathway: on protein death and cell life. EMBO J. **17:**7151–7160.
5. **Hershko, A., A. Ciechanover, and A. Varshavsky.** 2000. The ubiquitin system. Nat. Med. **6:**1073–1081.
6. **Jariel-Encontre, I., M. Pariat, F. Martin, S. Carillo, C. Salvat, and M. Piechaczyk.** 1995. Ubiquitinylation is not an absolute requirement for degradation of c-Jun protein by the 26 S proteasome. J. Biol. Chem. **270:**11623–11627.
7. **Jin, Y., H. Lee, S. X. Zeng, M. S. Dai, and H. Lu.** 2003. MDM2 promotes p21waf1/cip1 proteasomal turnover independently of ubiquitylation. EMBO J. **22:**6365–6377.
8. **Ju, D., and Y. Xie.** 2006. Identification of the preferential ubiquitination site and ubiquitin-dependent degradation signal of Rpn4. J. Biol. Chem. **281:**10657–10662.
9. **Lai, M. M. C., and C. F. Ware.** 1999. Hepatitis C virus core protein: possible roles in viral pathogenesis. Springer, Berlin, Germany.
10. **Lévy, F., N. Johnsson, T. Rumenapf, and A. Varshavsky.** 1996. Using ubiquitin to follow the metabolic fate of a protein. Proc. Natl. Acad. Sci. USA **93:**4907–4912.
11. **Li, X., L. Amazit, W. Long, D. M. Lonard, J. J. Monaco, and B. W. O'Malley.** 2007. Ubiquitin- and ATP-independent proteolytic turnover of p21 by the REGγ-proteasome pathway. Mol. Cell **26:**831–842.
12. **Li, X., D. M. Lonard, S. Y. Jung, A. Malovannaya, Q. Feng, J. Qin, S. Y. Tsai, M. J. Tsai, and B. W. O'Malley.** 2006. The SRC-3/AIB1 coactivator is degraded in a ubiquitin- and ATP-independent manner by the REGγ proteasome. Cell **124:**381–392.
13. **Liu, Q., C. Tackney, R. A. Bhat, A. M. Prince, and P. Zhang.** 1997. Regulated processing of hepatitis C virus core protein is linked to subcellular localization. J. Virol. **71:**657–662.
14. **Lonard, D. M., Z. Nawaz, C. L. Smith, and B. W. O'Malley.** 2000. The 26S proteasome is required for estrogen receptor-α and coactivator turnover and for efficient estrogen receptor-α transactivation. Mol. Cell **5:**939–948.
15. **Moradpour, D., F. Penin, and C. M. Rice.** 2007. Replication of hepatitis C virus. Nat. Rev. Microbiol. **5:**453–463.
16. **Moriishi, K., R. Mochizuki, K. Moriya, H. Miyamoto, Y. Mori, T. Abe, S. Murata, K. Tanaka, T. Miyamura, T. Suzuki, K. Koike, and Y. Matsuura.** 2007. Critical role of PA28γ in hepatitis C virus-associated steatogenesis and hepatocarcinogenesis. Proc. Natl. Acad. Sci. USA **104:**1661–1666.
17. **Moriishi, K., T. Okabayashi, K. Nakai, K. Moriya, K. Koike, S. Murata, T. Chiba, K. Tanaka, R. Suzuki, T. Suzuki, T. Miyamura, and Y. Matsuura.** 2003. Proteasome activator PA28γ-dependent nuclear retention and degradation of hepatitis C virus core protein. J. Virol. **77:**10237–10249.
18. **Niwa, H., K. Yamamura, and J. Miyazaki.** 1991. Efficient selection for high-expression transfectants with a novel eukaryotic vector. Gene **108:**193–199.
19. **Realini, C., C. C. Jensen, Z. Zhang, S. C. Johnston, J. R. Knowlton, C. P. Hill, and M. Rechsteiner.** 1997. Characterization of recombinant REGα, REGβ, and REGγ proteasome activators. J. Biol. Chem. **272:**25483–25492.
20. **Santolini, E., G. Migliaccio, and N. La Monica.** 1994. Biosynthesis and biochemical properties of the hepatitis C virus core protein. J. Virol. **68:**3631–3641.
21. **Sheaff, R. J., J. D. Singer, J. Swanger, M. Smitherman, J. M. Roberts, and B. E. Clurman.** 2000. Proteasomal turnover of p21Cip1 does not require p21Cip1 ubiquitination. Mol. Cell **5:**403–410.
22. **Shirakura, M., K. Murakami, T. Ichimura, R. Suzuki, T. Shimoji, K. Fukuda, K. Abe, S. Sato, M. Fukasawa, Y. Yamakawa, M. Nishijima, K. Moriishi, Y. Matsuura, T. Wakita, T. Suzuki, P. M. Howley, T. Miyamura, and I. Shoji.** 2007. E6AP ubiquitin ligase mediates ubiquitylation and degradation of hepatitis C virus core protein. J. Virol. **81:**1174–1185.
23. **Suzuki, R., K. Tamura, J. Li, K. Ishii, Y. Matsuura, T. Miyamura, and T. Suzuki.** 2001. Ubiquitin-mediated degradation of hepatitis C virus core protein is regulated by processing at its carboxyl terminus. Virology **280:**301–309.
24. **Suzuki, T., and A. Varshavsky.** 1999. Degradation signals in the lysine-asparagine sequence space. EMBO J. **18:**6017–6026.
25. **Treier, M., L. M. Staszewski, and D. Bohmann.** 1994. Ubiquitin-dependent c-Jun degradation in vivo is mediated by the δ domain. Cell **78:**787–798.
26. **Wu, R. C., Q. Feng, D. M. Lonard, and B. W. O'Malley.** 2007. SRC-3 coactivator functional lifetime is regulated by a phospho-dependent ubiquitin time clock. Cell **129:**1125–1140.
27. **Zhang, Z., and R. Zhang.** 2008. Proteasome activator PA28γ regulates p53 by enhancing its MDM2-mediated degradation. EMBO J. **27:**852–864.

JOURNAL OF VIROLOGY, Aug. 2008, p. 7964–7976 Vol. 82, No. 16
0022-538X/08/$08.00+0 doi:10.1128/JVI.00826-08

Interaction of Hepatitis C Virus Nonstructural Protein 5A with Core Protein Is Critical for the Production of Infectious Virus Particles[▽]

Takahiro Masaki,[1] Ryosuke Suzuki,[1] Kyoko Murakami,[1] Hideki Aizaki,[1] Koji Ishii,[1] Asako Murayama,[1] Tomoko Date,[1] Yoshiharu Matsuura,[2] Tatsuo Miyamura,[1] Takaji Wakita,[1] and Tetsuro Suzuki[1]*

Department of Virology II, National Institute of Infectious Diseases, Shinjuku-ku, Tokyo 162-8640, Japan,[1] and Department of Molecular Virology, Research Institute for Microbial Diseases, Osaka University, Suita-shi, Osaka 565-0871, Japan[2]

Received 17 April 2008/Accepted 22 May 2008

Nonstructural protein 5A (NS5A) of the hepatitis C virus (HCV) possesses multiple and diverse functions in RNA replication, interferon resistance, and viral pathogenesis. Recent studies suggest that NS5A is involved in the assembly and maturation of infectious viral particles; however, precisely how NS5A participates in virus production has not been fully elucidated. In the present study, we demonstrate that NS5A is a prerequisite for HCV particle production as a result of its interaction with the viral capsid protein (core protein). The efficiency of virus production correlated well with the levels of interaction between NS5A and the core protein. Alanine substitutions for the C-terminal serine cluster in domain III of NS5A (amino acids 2428, 2430, and 2433) impaired NS5A basal phosphorylation, leading to a marked decrease in NS5A-core interaction, disturbance of the subcellular localization of NS5A, and disruption of virion production. Replacing the same serine cluster with glutamic acid, which mimics the presence of phosphoserines, partially preserved the NS5A-core interaction and virion production, suggesting that phosphorylation of these serine residues is important for virion production. In addition, we found that the alanine substitutions in the serine cluster suppressed the association of the core protein with viral genome RNA, possibly resulting in the inhibition of nucleocapsid assembly. These results suggest that NS5A plays a key role in regulating the early phase of HCV particle formation by interacting with core protein and that its C-terminal serine cluster is a determinant of the NS5A-core interaction.

Hepatitis C virus (HCV) infection is a major public health problem and is prevalent in about 200 million people worldwide (27, 40, 42). Current protocols for treating HCV infection fail to produce a sustained virological response in as many as half of treated individuals, and many cases progress to chronic liver disease, including chronic hepatitis, cirrhosis, and hepatocellular carcinoma (15, 31, 35, 43).

HCV is a positive-strand RNA virus classified in the *Hepacivirus* genus within the *Flaviviridae* family (55). Its approximately 9.6-kb genome is translated into a single polypeptide of about 3,000 amino acids (aa), in which the structural proteins core, E1, and E2 reside in the N-terminal region. A crucial function of core protein is assembly of the viral nucleocapsid. The amino acid sequence of this protein is well conserved among different HCV strains compared to other HCV proteins. The nonstructural (NS) proteins NS3-NS5B are considered to assemble into a membrane-associated HCV RNA replicase complex. NS3 possesses the enzymatic activities of serine protease and RNA helicase, and NS4A serves as a cofactor for NS3 protease. NS4B plays a role in the remodeling of host cell membranes, probably to generate the site for the replicase assembly. NS5B functions as the RNA-dependent RNA polymerase. NS5A is known to play an important but undefined role in viral RNA replication.

NS5A is a phosphoprotein that can be found in basally phosphorylated (56 kDa) and hyperphosphorylated (58 kDa) forms (49). Comparative sequence analyses and limited proteolysis of recombinant NS5A have demonstrated that NS5A is composed of three domains (52). Domain I is relatively conserved among HCV genotypes compared to domains II and III. Analysis of the crystal structure of the conserved domain I that immediately follows the membrane-anchoring α-helix localized at the N terminus revealed a dimeric structure (53). The interface between protein molecules is characterized by a large, basic groove, which has been proposed as a site of RNA binding. In fact, its RNA binding property has been demonstrated biochemically (17). Domains II and III of NS5A are far less understood. Domain II contains a region referred to as the interferon sensitivity determining region, and this region and its C-terminal 26 residues have been shown to be essential for interaction with the interferon-induced, double-stranded RNA-dependent protein kinase (6–10, 38, 39, 48). Domain III includes a number of potential phosphoacceptor sites and is most likely involved in basal phosphorylation. This domain tolerates insertion of large heterologous sequences such as green fluorescent protein (GFP) and is not required for function of NS5A in HCV RNA replication (1, 34). However, a study with the recently established productive HCV cell culture system using genotype 2a isolate JFH-1 (28, 56, 58) demonstrated that while insertion of GFP within the NS5A region does not affect RNA replication, it does produce marked decreases in the production of infectious virus particles (41). This suggests that the C-terminal region of NS5A may affect virus particle production independent of RNA replication. Re-

* Corresponding author. Mailing address: Department of Virology II, National Institute of Infectious Diseases, 1-23-1 Toyama, Shinjuku-ku, Tokyo 162-8640, Japan. Phone: 81 3 5285 1111. Fax: 81 3 5285 1161. E-mail: tesuzuki@nih.go.jp.

▽ Published ahead of print on 4 June 2008.

cently, Miyanari et al. reported that the association of core protein with the NS proteins and replication complexes around lipid droplets (LDs) is critical for producing infectious viruses (33).

In the present study, we demonstrated that NS5A is a prerequisite for HCV particle production via its interaction with core protein, and we identified serine residues in the C-terminal region of NS5A that play an important role in virion production. Substitution of the serine residues with alanine residues inhibited not only the interaction of NS5A with core protein but also HCV RNA-core association and led to a decrease in HCV particle production with no effect on RNA replication.

MATERIALS AND METHODS

DNA construction. Plasmids pJFH1, which contains the full-length JFH-1 cDNA downstream of the T7 RNA promoter sequence, and pSGR-JFH1/Luc, in which the neomycin resistance gene of pSGR-JFH1 has been replaced by the firefly luciferase reporter gene, have been previously described (24, 56). To generate the fluorochrome gene-tagged full-length JFH-1 plasmid, pJFH1/NS5A-GFP, the region encompassing the RsrII site of NS5A and the BsrGI site of NS5B was amplified by PCR, the amplification product was cloned into pGEM-T Easy vector (Promega, Madison, WI), and the resultant plasmid was designated pGEM-JFH1/RsrII-BsrGI. A GFP reporter gene was amplified by PCR from pGreen Lantern-1 (Invitrogen, Carlsbad, CA) with primers containing the XhoI sequence and inserted, after restriction digestion with XhoI, into the XhoI site of pGEM-JFH1/RsrII-BsrGI. The resulting plasmid was digested by RsrII and BsrGI and ligated into pJFH1 similarly digested by RsrII and BsrGI to produce pJFH1/NS5A-GFP. For generation of the fluorochrome gene-tagged subgenomic reporter plasmid, pJFH1/NS5A-GFP was digested by RsrII and SnaBI and ligated into pSGR-JFH1/Luc similarly digested by RsrII and SnaBI. The mutations in the NS5A gene were generated by oligonucleotide-directed mutagenesis (57). To construct plasmids expressing N-terminally FLAG-tagged HCV core protein or hemagglutinin (HA)-tagged NS5A, DNA fragments encoding core protein or NS5A (wild type or mutants) were generated from the full-length JFH-1 cDNA by PCR. The core protein coding sequence, together with a FLAG sequence linked to its N terminus, was cloned into the pCAGGS vector (37). The coding sequences of NS5A, together with an HA sequence linked to their N termini, were also cloned into pCAGGS vectors. All PCR products were confirmed by automated nucleotide sequencing with an ABI Prism 3130 Avant Genetic Analyzer (Applied Biosystems, Tokyo, Japan).

Cells and viruses. The human hepatoma cell line, Huh-7, and JFH1/4-1 cells, which are Huh-7 cells carrying a subgenomic replicon of JFH-1 (32), were maintained in Dulbecco's modified Eagle's medium (DMEM) supplemented with minimal essential medium nonessential amino acids (Invitrogen), 100 units/ml of penicillin, 100 μg/ml of streptomycin, and 10% fetal bovine serum (FBS) at 37°C in a 5% CO_2 incubator. Huh/c-p7 cells, which are Huh-7 cells stably expressing the proteins core to p7 derived from the JFH-1 strain (18), were incubated in DMEM containing 300 μg/ml of zeocin (Invitrogen). HCV particles derived from JFH-1 were produced by transient transfection of Huh-7 cells with in vitro transcribed RNA, as described previously (56, 58). Recombinant vaccinia virus strain DIs, which expresses the bacteriophage T7 RNA polymerase under the control of the vaccinia virus early/late promoter P7.5, was generated and propagated as previously described (19).

DNA transfection, immunoprecipitation (IP), and immunoblotting. For coexpression of FLAG-tagged core protein and HA-tagged NS5A, cells were seeded onto 35-mm wells of a six-well cell culture plate and cultured overnight. Plasmid DNAs (2 μg) were transfected into cells using TransIT-LT1 transfection reagent (Mirus, Madison, WI). Cells were harvested at 48 h posttransfection, washed three times with 1 ml of ice-cold phosphate-buffered saline (PBS), and suspended in 0.25 ml lysis buffer (20 mM Tris-HCl [pH 7.4] containing 135 mM NaCl, 1% Triton X-100, 0.05% sodium dodecyl sulfate [SDS], and 10% glycerol) supplemented with 50 mM NaF, 5 mM Na_3VO_4, 1 μg/ml leupeptin, and 1 mM phenylmethylsulfonyl fluoride (PMSF). Cell lysates were sonicated at 4°C for 5 min, incubated for 30 min at 4°C, and centrifuged at 14,000 × *g* for 5 min at 4°C. After preclearing, the supernatant was immunoprecipitated with 10 μl of anti-FLAG M2-agarose beads (Sigma, St. Louis, MO). For expression of the full-length HCV polyprotein, Huh-7 cells transfected with 10 μg of in vitro transcribed RNAs by electroporation were resuspended in 20 or 30 ml of culture medium, and 10-ml aliquots were seeded into 100-mm culture dishes. At 72 h posttransfection, the cells were incubated in 0.5 ml of lysis buffer (20 mM Tris-HCl [pH 7.4] containing 135 mM NaCl, 1% Triton X-100, 0.5% sodium deoxycholate, and 10% glycerol) supplemented with 50 mM NaF, 5 mM Na_3VO_4, 1 μg/ml leupeptin, and 1 mM PMSF. After preclearing, the supernatant was immunoprecipitated with 5 μg of polyclonal anti-NS5A antibody (34a) or polyclonal anti-C/EBPβ antibody (Santa Cruz Biotechnology, Santa Cruz, CA), and 20 μl of protein G-agarose beads (Invitrogen). The immunocomplex was precipitated with the beads by centrifugation at 800 × *g* for 30 s and then was washed five times with lysis buffer by centrifugation. The proteins binding to the beads were boiled in 20 μl of SDS sample buffer and then subjected to SDS–12.5% polyacrylamide gel electrophoresis (PAGE). The proteins were transferred onto a polyvinylidene difluoride membrane (Immobilon; Millipore, Bedford, MA) and then reacted with a primary antibody and a secondary horseradish peroxidase-conjugated antibody. The immunocomplexes were visualized with an ECL Plus Western Blotting Detection System (GE Healthcare, Buckinghamshire, United Kingdom) and detected using an LAS-3000 imaging analyzer (Fujifilm, Tokyo, Japan).

In vitro synthesis of HCV RNA and RNA transfection. Plasmid DNAs were digested with XbaI and treated with mung bean nuclease (New England Biolabs, Ipswich, MA) to remove the four terminal nucleotides, resulting in the correct 3′ end of the HCV cDNA. Digested DNAs were purified and used as templates for RNA synthesis. HCV RNA was synthesized in vitro using a MEGAscript T7 kit (Ambion, Austin, TX). Synthesized RNA was treated with DNase I (Ambion), followed by acid guanidinium thiocyanate-phenol-chloroform extraction to remove any remaining template DNA. Synthesized HCV RNAs were used for electroporation. Trypsinized Huh-7 cells were washed with Opti-MEM I reduced-serum medium (Invitrogen) and resuspended at 3 × 10^6 cells/ml with Cytomix buffer (54). RNA was mixed with 400 μl of cell suspension and transferred into an electroporation cuvette (Precision Universal Cuvettes; Thermo Hybaid, Middlesex, United Kingdom). Cells were then pulsed at 260 V and 950 μF using a Gene Pulser II unit (Bio-Rad, Hercules, CA). Transfected cells were immediately transferred onto six-well culture plates or 100-mm culture dishes.

Luciferase assay. Cells were harvested at different time points posttransfection of subgenomic reporter replicons and lysed in passive lysis buffer (Promega). The luciferase activity in cells was determined using a luciferase assay system (Promega).

Quantification of HCV core protein. HCV core protein in transfected cells or cell culture supernatants was quantified using a highly sensitive enzyme immunoassay (Ortho HCV antigen ELISA Kit; Ortho Clinical Diagnostics, Tokyo, Japan). To determine intracellular core protein amounts, cell lysates were prepared as described previously (41). To determine the efficiency of core protein release, the ratio of extracellular core protein to total core protein (the sum of intra- and extracellular core protein amounts) was calculated.

Intra- and extracellular infectivity assay. Culture supernatants were harvested 72 h posttransfection, and virus titers were determined by a 50% tissue culture infectious dose ($TCID_{50}$) assay as described previously (28, 46). Virus titration was performed by seeding naïve Huh-7 cells in 96-well plates at a density of 1 × 10^4 cells/well. Samples were serially diluted fivefold in complete growth medium and used to infect the seeded cells (six wells per dilution). At 72 h after infection, the inoculated cells were fixed and immunostained with a mouse monoclonal anti-core protein antibody (2H9) (56), followed by an Alexa Fluor 488-conjugated anti-mouse immunoglobulin G (IgG) (Invitrogen). Wells that showed at least one core protein-expressing cell was counted as positive. Cell-associated infectivity was determined essentially as described previously (12, 47). Briefly, cells were extensively washed with PBS, scraped, and centrifuged for 3 min at 120 × *g*. Cell pellets were resuspended in 1 ml of DMEM containing 10% FBS and subjected to four cycles of freezing and thawing using dry ice and a 37°C water bath. Samples were then centrifuged at 2,400 × *g* for 10 min at 4°C to remove cell debris, and cell-associated infectivity was determined by $TCID_{50}$ assay.

Expression of HCV proteins using vaccinia viruses, metabolic labeling of cells, and radioimmunoprecipitation analysis. Metabolic labeling of cells and radioimmunoprecipitation analysis were performed as described by Huang et al. (17) with some modifications. A total of 4 × 10^5 Huh-7 cells were seeded onto each well of six-well cell culture plates and cultured overnight. A 2-μg amount of subgenomic replicon DNAs carrying defined NS5A mutations was transfected into cells using TransIT-LT1 transfection reagent, and at 12 h posttransfection the cells were then infected at a multiplicity of infection of 10 with recombinant vaccinia viruses expressing the T7 RNA polymerase. After 40 h of transfection, cells were incubated in methionine- and cysteine-deficient DMEM (Invitrogen) or phosphate-deficient DMEM (Invitrogen) for 2 h and labeled for 6 h with [^{35}S]methionine and [^{35}S]cysteine (200 μCi/well; GE Healthcare) or

[^{32}P]orthophosphate (250 μCi/well; GE Healthcare). The cells were then washed twice with cold PBS and lysed with SDS lysis buffer (50 mM Tris-HCl [pH 7.6], 0.5% SDS, 1 mM EDTA, 20 μg/ml of PMSF). The cell lysates were passed through a 27-gauge needle several times to shear cellular DNA. After a 10-min incubation at 75°C, the lysates were clarified by centrifugation and diluted fivefold with HNAET buffer (50 mM HEPES [pH 7.5], 150 mM NaCl, 0.67% bovine serum albumin, 1 mM EDTA, 0.33% Triton X-100). After preclearing by incubation with 20 μl of protein G-agarose beads for 1 h at 4°C, the supernatant was incubated with 2 μg of rabbit polyclonal anti-NS5A antibody overnight at 4°C. A 20-μl aliquot of protein G agarose beads was further added and incubated for 2 h at 4°C. The cell pellets were washed three times with 0.5 ml of HNAETS buffer (HNAET containing 0.5% SDS), followed by washing once with 0.5 ml of HNE buffer (50 mM HEPES [pH 7.5], 150 mM NaCl and 1 mM EDTA). After treatment with or without λ protein phosphatase (New England Biolabs), the cell pellets were suspended in 20 μl of SDS sample buffer and boiled for 10 min. The proteins were resolved on 10% SDS-polyacrylamide gels and analyzed by autoradiography.

Subcellular fractionation analysis. All steps were carried out at 4°C in the presence of a protease inhibitor cocktail (Complete; Roche, Mannheim, Germany) as described previously (20), with some modifications. Cells were suspended in four cell volumes of homogenization buffer (50 mM NaCl, 10 mM triethylamine [pH 7.4], 1 mM EDTA), snap frozen in liquid nitrogen, stored at −80°C, and thawed in a water bath at room temperature. Supernatants (0.4 ml) were layered on linear 10-ml iodixanol gradients from 2.5 to 25% and centrifuged at 37,000 rpm for 3.5 h in an SW41 rotor (Beckman, Fullerton, CA), followed by collection of 0.8-ml fractions from the top. Each fraction was concentrated by Centricon YM30 (Millipore), separated by SDS-PAGE, and immunoblotted with a rabbit polyclonal anti-calnexin antibody (Stressgen Biotechnologies, Victoria, Canada), a mouse monoclonal anti-adipose differentiation-related protein (ADRP) antibody (Progen Biotechnik, Heidelberg, Germany), or a rabbit polyclonal anti-NS5A antibody. The core protein amount in each fraction was also determined by enzyme-linked immunosorbent assay (ELISA).

IP-RT-PCR. The process of cell lysis to RNA purification was carried out essentially as described by Johnson et al. (21) with some modifications. A total of 3×10^6 Huh-7 cells were transfected with 10 μg of in vitro transcribed HCV RNAs and resuspended in 20 or 30 ml of culture medium, after which 10-ml aliquots were seeded into 100-mm culture dishes. At 72 h posttransfection, the cells were scraped and incubated in 500 μl of hypotonic buffer (10 mM HEPES [pH 7.6], 1.5 mM $MgCl_2$, 10 mM KCl, 0.2 mM PMSF) per dish. The cells were passed through a 20-gauge needle several times, lysed with Nonidet P-40 at a final concentration of 1%, and incubated on ice for an additional 10 min. After centrifugation at 4,000 × *g* at 4°C for 15 min, glycerol was added to the supernatants at a final concentration of 5%. The cell lysates were incubated with 20 μl of protein G-agarose beads for 30 min at room temperature. After the cell lysates were removed from protein G-agarose beads, 5 μg of mouse monoclonal anti-core protein antibody or normal mouse IgG (Sigma) as a negative control was added, and samples were incubated for an additional 1 h at room temperature. A 20-μl aliquot of protein G-agarose beads per sample was added to the cell lysates and incubated for 1 h. After incubation, the beads were washed three times with wash buffer (10 mM Tris-HCl [pH 7.6], 100 mM KCl, 5 mM $MgCl_2$, and 1 mM dithiothreitol) and eluted in 100 μl of elution buffer (50 mM Tris-HCl [pH 8.0], 1% SDS, and 10 mM EDTA) at 65°C for 10 min. After treatment with 100 μg of proteinase K at 37°C for 30 min, the RNAs in immunocomplexes were isolated by acid guanidinium thiocyanate-phenol-chloroform extraction. Reverse transcriptase PCR (RT-PCR) was carried out using random hexamer and Superscript II RT (Invitrogen), followed by nested PCR with LA *Taq* DNA polymerase (TaKaRa, Shiga, Japan) and primer sets amplifying the fragments of nucleotides (nt) 129 to 2367 and nt 7267 to 9463 of the JFH-1 genome. To amplify the fragment of nt 129 to 2367, the sense primer 5′-CTGTGAGGAACTACTGTCTT-3′ and the antisense primer 5′-TCCACGATGTTCTGGTGAAG-3′ were used for first-round PCR; the sense primer 5′-CGGGAGAGCCATAGTGG-3′ and the antisense primer 5′-CATTCCGTGGTAGAGTGCA-3′ were used for second-round PCR. To amplify the fragment of nt 7267 to 9463, the sense primer 5′-GTCCAGGGTGCCCGTTCTGGACT-3′ and the antisense primer 5′-GCGGCTCACGGACCTTTCAC-3′ were used for first-round PCR; the sense primer 5′-CACCGTTGCTGGTTGTGCT-3′ and the antisense primer 5′-GTGTACCTAGTGTGTGCCGCTCTA-3′ were used for second-round PCR.

Indirect immunofluorescence analysis. Cells incubated for 3 days after transfection with JFH-1 RNAs were seeded in an eight-well chamber slide (BD Biosciences, San Jose, CA) and cultured overnight. The adherent cells were washed twice with PBS and fixed with 4% paraformaldehyde at room temperature. After a washing step with PBS, the cells were permeabilized with PBS containing 0.3% Triton X-100 and 2% FBS for 1 h at room temperature and stained with a rabbit polyclonal anti-NS5A antibody and a mouse monoclonal anti-core protein antibody. The fluorescent secondary antibodies were Alexa Fluor 488- or Alexa Fluor 555-conjugated anti-rabbit or anti-mouse IgG antibodies (Invitrogen). Analyses of JFH-1 were performed on a Zeiss confocal laser scanning microscope LSM 510 (Carl Zeiss, Oberkochen, Germany).

RESULTS

Mutations of serine residues at the NS5A C terminus impair basal phosphorylation but have little effect on viral RNA replication. As demonstrated in a previous study, insertion of GFP into the NS5A C terminus does not significantly affect viral RNA replication but reduces the generation of infectious HCV particles (41). The C-terminal region of NS5A contains highly conserved serine residues that are involved in basal phosphorylation (1, 23, 49). To examine the involvement of the serine clusters (cluster 3-A [CL3A] and cluster 3-B [CL3B]) in the C-terminal region of NS5A in HCV particle production, we created mutated HCV genomes as well as subgenomic replicons carrying alanine substitutions for the conserved serine residues at aa 2384, 2388, 2390, and 2391 (residues are numbered according to the positions within the original JFH-1 polyprotein) (CL3A/SA); at aa 2428, 2430, and 2433 (CL3B/SA); or an in-frame deletion spanning aa 2384 to 2433 (Δ2384–2433) (Fig. 1). A construct with an in-frame insertion of GFP (NS5A-GFP) was also generated as described previously for the Con1 isolate (34).

First, we analyzed the effects of the NS5A mutations on HCV RNA replication using a transient RNA replication assay using subgenomic luciferase reporter replicons (Fig. 2A) and found that the serine-to-alanine substitutions (CL3A/SA and CL3B/SA) did not affect viral RNA replication. NS5A-GFP and Δ2384–2433 slightly reduced RNA replication, indicating that the mutations of the NS5A C terminus tested in this study do not critically affect RNA replication, which is consistent with previous reports (1, 34, 51).

Next, the phosphorylation status of the mutated NS5A was analyzed as described in Materials and Methods (Fig. 2B). NS5A was isolated from radiolabeled cells by IP and analyzed either directly by SDS-PAGE or after treatment with λ protein phosphatase. Analysis of ^{32}P-radiolabeled proteins revealed that the CL3A/SA, CL3B/SA, and Δ2384–2433 mutations resulted in marked reduction of basal phosphorylation (Fig. 2B, compare lane 1 with lanes 3, 5, and 7 in the top panel). All ^{32}P-labeled NS5A proteins were sensitive to treatment with phosphatase (lanes 2, 4, 6, and 8). The possibility that loss of signal after dephosphorylation was due to contaminating proteases present in the phosphatase preparations can be ruled out because no degradation of the ^{35}S-labeled proteins was observed (Fig. 2B, bottom panel). These results suggest that mutations in the C-terminal serine cluster of NS5A impair basal phosphorylation but have no significant effect on viral RNA replication.

Effect of mutations introduced into the NS5A C terminus on the production of infectious HCV particles. To analyze HCV particle production from cells transfected with the in vitro transcribed viral genomic RNAs, we harvested supernatants and cells at 4, 24, 48, 72, and 96 h posttransfection and measured the amounts of core protein. As shown in Fig. 3A, comparable amounts of core proteins were detected in all transfected cells 4 h after transfection, reflecting unchanged

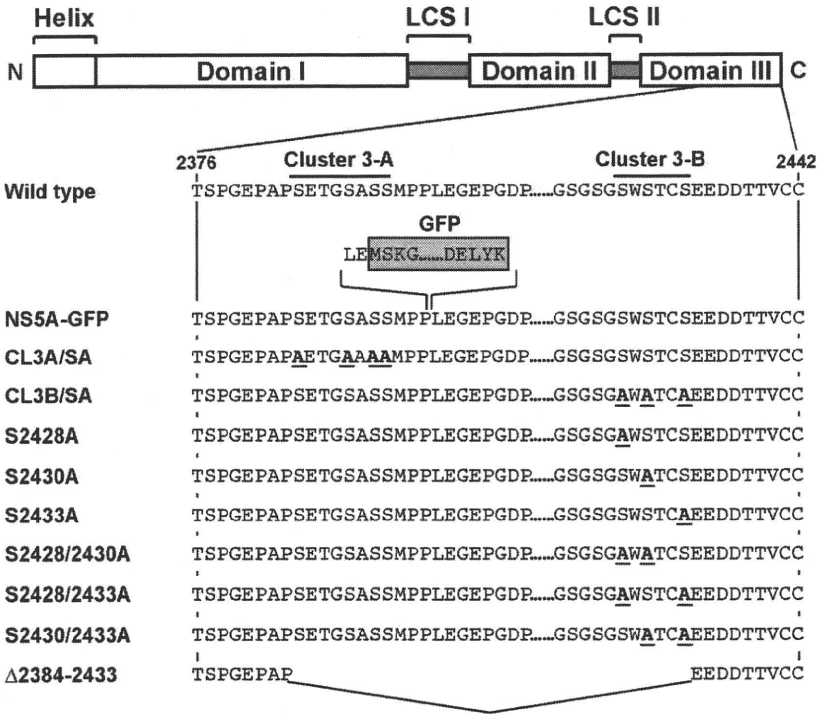

FIG. 1. Structures of HCV constructs used in this study. Schematic diagram of the NS5A structure according to Tellinghuisen et al. (52) is shown in the top panel. The three domains are indicated by white boxes and are separated by trypsin-sensitive regions with presumably low structural complexity (low-complexity sequence [LCS]). The numbers indicate amino acid residues within the original JFH-1 polyprotein. The names listed on the left represent full-length HCV constructs, subgenomic reporter replicons, or N-terminally HA-tagged NS5A constructs used in this study. NS5A-GFP carries a GFP insertion between aa 2394 and 2395 as indicated by a shaded box. CL3A/SA and CL3B/SA carry several serine-to-alanine substitutions in the NS5A C terminus constructed as described previously (1). HCV constructs from S2428A to S2430/2433A carry single or double serine-to-alanine substitutions generated by modification of the CL3B/SA construct. The Δ2384–2433 mutant possesses an in-frame deletion in the C-terminal region of NS5A. Amino acid substitutions are marked in bold and underlined. N and C represent N terminus and C terminus, respectively.

transfection efficiencies, and the kinetics of intracellular core protein levels was similar among transfectants. By contrast, core protein released from cells transfected either with the mutated genome of CL3B/SA, Δ2384–2433, or NS5A-GFP was more than 10-fold lower than that for the wild-type JFH-1 or CL3A/SA (Fig. 3B). Figure 3C shows the efficiency of core protein release from each transfectant, which is expressed as a percentage of the extracellular core protein level relative to the amount of total core protein (the sum of intra- and extracellular core protein). Core protein release efficiency with the wild type and CL3A/SA was 2 to 13% at 48 to 96 h after transfection, while only 1% or less of core protein was released in the cases of CL3B/SA, Δ2384–2433, and NS5A-GFP strains.

To further investigate production and release of infectious virus particles, naïve Huh-7 cells were infected with culture supernatants of cells harvested 72 h posttransfection, and infectious virus titers were determined by $TCID_{50}$ assay at 72 h after infection. Figure 3D shows that release of infectious virus particles from cells transfected with the genome of CL3B/SA or Δ2384–2433 mutants was markedly reduced (about 10,000-fold) compared to that from wild-type- or CL3A/SA-transfected cells (white bars). To examine whether such a decrease in infectious HCV in the culture supernatants was attributable to defective virion assembly or impaired release of virions, we determined cell-associated infectivity (Fig. 3D). Production of intracellular infectious virions in CL3B/SA- and Δ2384-2433-transfected cells was strongly impaired in comparison with that in wild-type-transfected (~1,000-fold) and CL3A/SA-transfected (~100-fold) cells. Thus, the results suggest a potential role for the serine cluster at aa 2428, 2430, and 2433 of NS5A in assembly of infectious HCV particles. Among the NS5A mutations tested, CL3B/SA is of particular interest because this mutation leads to a marked reduction in HCV production with no impact on viral RNA replication.

Serine residues at aa 2428, 2430, and 2433 are important for the interaction between NS5A and core protein. Miyanari et al. reported that the association of core protein with NS proteins is critical for infectious HCV production and that mutations of the core protein and NS5A that cause these proteins to fail to associate with each other impair the production of infectious virus (33). Based on these observations and the findings noted above, we hypothesize that NS5A plays a key role in recruiting viral RNA, which is synthesized at the viral replication complex, to nucleocapsid formation via interaction between the NS5A C-terminal region and the core protein. To prove this, we analyzed the interaction of NS5A with the core protein by coimmunoprecipitation experiments. HA-tagged NS5A constructs carrying defined mutations were generated (Fig. 1) and coexpressed with the FLAG-tagged core protein in Huh-7 cells. As shown in Fig. 4A, coimmunoprecipitation of NS5A

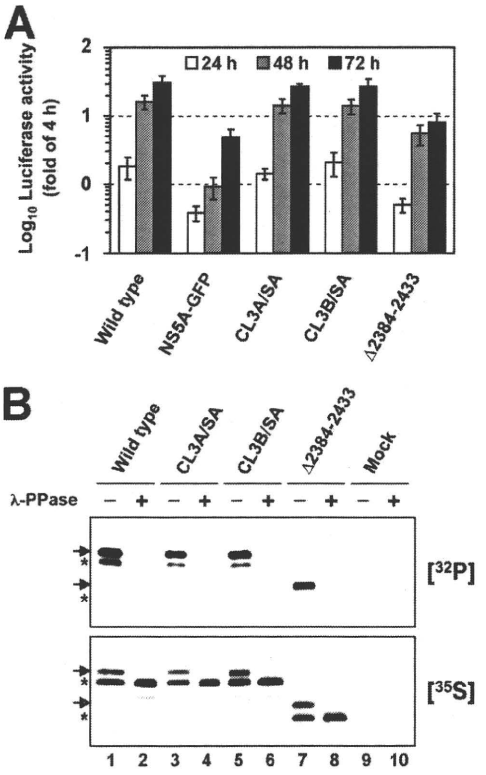

FIG. 2. Mutations at the C terminus of NS5A impair basal phosphorylation and have only a minor impact on RNA replication. (A) Replication of given mutants in transfected Huh-7 cells as determined by luciferase reporter assays performed at 24, 48, and 72 h posttransfection (white, gray, and black bars, respectively). Values given were normalized for transfection efficiency using the luciferase activity determined 4 h after transfection, which was set to 1. Mean values of quadruplicate measurements and the standard deviations are given. (B) Phosphorylation analysis of NS5A using the vaccinia virus T7 hybrid system. NS3-to-NS5B polyprotein fragments carrying the mutations specified above the lanes were transfected into Huh-7 cells, and proteins were radiolabeled with [^{32}P]orthophosphate or [^{35}S]methionine and [^{35}S]cysteine. NS5A proteins were isolated by IP and separated by SDS-PAGE (10% polyacrylamide). Mock-transfected cells served as a negative control (lanes 9 and 10). Half of the samples were treated with λ protein phosphatase (λ-PPase) (+) whereas the other half was mock treated (−) prior to SDS-PAGE. Arrows and asterisks indicate hyperphosphorylated and basally phosphorylated forms, respectively.

with the core protein was observed in cells expressing the wild-type NS5A and the CL3A/SA-mutated NS5A, but the amount of immunoprecipitated NS5A in the CL3A/SA-expressing cells was slightly lower than that in the wild-type-expressing cells. In contrast, the CL3B/SA- or the Δ2384-2433-mutated NS5A coimmunoprecipitated with the core protein only slightly or not at all.

We further examined the interaction of NS5A with core protein in cells expressing HCV genomes. At 72 h posttransfection with the wild type or CL3B/SA, cells were harvested and immunoprecipitated with an anti-NS5A antibody or an anti-C/EBPβ antibody as a negative control, followed by immunoblotting. Under these experimental conditions, the amount of extracellular core protein released from cells transfected with the CL3B/SA genome was about 10-fold lower than that for the wild type, although comparable amounts of intracellular core protein were observed in both transfectants (Fig. 4B, left panels). As shown in the right panels of Fig. 4B, the core protein was specifically coimmunoprecipitated with NS5A in cells expressing the wild-type JFH-1 genome but not with the mutated NS5A in cells expressing the CL3B/SA genome. These results demonstrate that NS5A interacts with the core protein in cells producing infectious particles and that serine residues at aa 2428, 2430, and 2433 are important to the success of this interaction.

Two serine residues among aa 2428, 2430, and 2433 are responsible for regulating the interaction of NS5A with the core protein as well as HCV particle production. To further determine the critical residues in the C-terminal serine cluster of NS5A responsible for HCV particle production, we replaced one or two serine residues in the region with alanine (Fig. 1) and investigated which serine-to-alanine substitution influenced HCV particle production. Core protein levels in cells transfected with any construct were comparable over 4 days after transfection, indicating similar efficiencies of transfection and RNA replication from each construct (data not shown). As shown in Fig. 5A, we observed a slight delay in the kinetics of core protein release from cells transfected with the single-substitution genomes, S2428A, S2430A, and S2433A, up to 48 or 72 h posttransfection. However, core protein release from these cells reached comparable levels to that for the wild type at 96 h after transfection. In the cases of the double-substitution mutants (Fig. 5B), core protein release from cells transfected with the double-substitution genomes was markedly reduced, with 10- to 30-fold decreases compared to that for wild type observed. The kinetics of core protein release were similar to that for CL3B/SA.

Interaction of NS5A carrying single or double serine-to-alanine substitutions with the core protein was investigated by coimmunoprecipitation analysis using HA-tagged NS5A constructs. NS5A mutants carrying a single substitution were coimmunoprecipitated with the core protein (Fig. 5C), while none of the double-substitution NS5A mutants or the triple-substitution mutant, CL3B/SA, coimmunoprecipitated with the core protein (Fig. 5D). These results suggest that at least two serine residues in the C-terminal serine cluster of NS5A (aa 2428, 2430, and 2433) are necessary for the interaction between NS5A and the core protein as well as for regulation of HCV particle production and that there is positive correlation between their interaction and the amount of core protein released.

Glutamic acid partially substitutes for serine phosphorylation in the interaction of NS5A with the core protein and virus production. A consequence of phosphorylation is the addition of negative charge to a protein. In some cases, phosphoserine can be mimicked by glutamic or aspartic acid (14). To determine whether the introduction of negative charges into aa 2428, 2430, and 2433 instead of phosphoserines positively regulates the interaction of NS5A with the core protein and virus production, we replaced the serine residues with glutamic acid residues and constructed the CL3B/SE and S2428/2430E mutants (Fig. 6A). Cells transfected with the double-glutamic acid substitution, S2428/2430E, exhibited similar kinetics to the wild-type-transfected cells and released ~22-fold more core protein than S2428/2430A-transfected cells by 96 h posttransfection (Fig. 6B). In contrast,

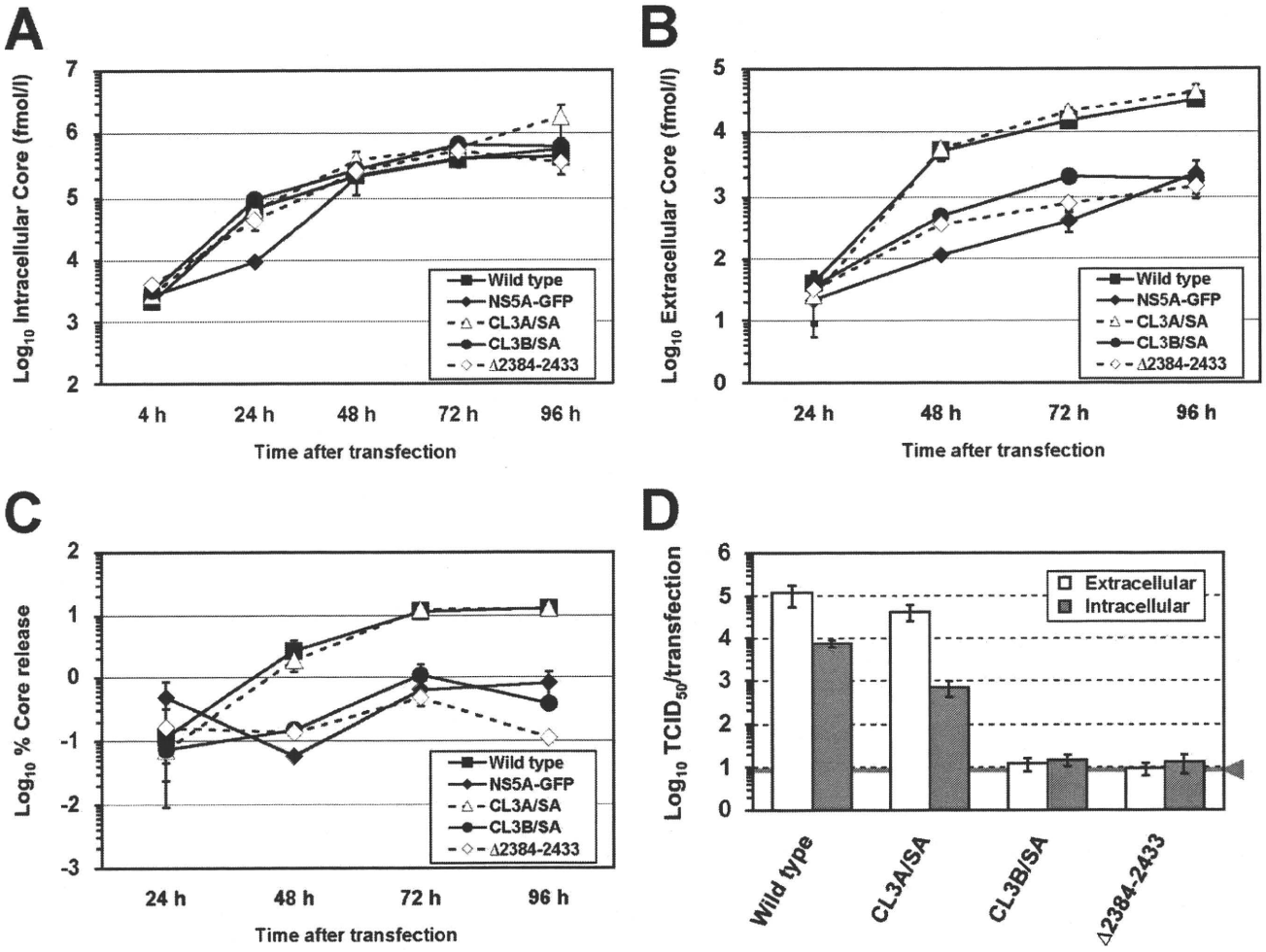

FIG. 3. Effect of mutations introduced into the NS5A C terminus on the production of infectious HCV particles. (A) Intracellular levels of core protein measured at various time points after transfection. A total of 3×10^6 Huh-7 cells were transfected with 10 μg of in vitro-transcribed HCV RNAs specified in the inset and resuspended in 10 ml of culture medium, after which 2-ml aliquots were seeded into each well of a six-well culture plate. The cells were harvested at different time points between 4 h and 96 h posttransfection, and then 500 μl of cell lysate per well was prepared. After centrifugation, supernatants were processed for a core protein-specific ELISA. (B) Release of core protein from cells transfected with the HCV genomes specified in the inset. Cell culture supernatants harvested from cells given in panel A were analyzed by a core protein ELISA. (C) Efficiency of core protein release from cells transfected with the HCV genomes specified in the inset. The percent core protein release (vertical axis) indicates the percentage of released core protein in relation to total core protein (the sum of intra- and extracellular core protein) calculated for each time point. (D) Infectivity of virus particles contained in supernatants and cells after transfection with mutants specified below the graph. Culture supernatants and cells were harvested 72 h posttransfection, and extracellular (white bars) and intracellular infectivity (gray bars) levels were determined by $TCID_{50}$ assay. The gray line and arrowhead represent the detection limit of the limiting dilution assay. Mean values and standard deviations for at least triplicates are shown in all panels.

the transfectant with the triple glutamic acid substitution, CL3B/SE, showed similar trends to that of CL3B/SA. In the coimmunoprecipitation experiments with FLAG-tagged core protein and HA-tagged NS5A constructs (Fig. 6C), S2428/2430E, but not S2428/2430A, restored the ability of NS5A to interact with the core protein up to a similar level to that of wild type. As expected, neither CL3B/SE nor CL3B/SA coimmunoprecipitated with the core protein. Taken together, these results indicate that negative charges at aa 2428 and 2430 preserve the ability of NS5A to interact with the core protein and positively regulate virus production. However, the data of the CL3B/SE mutant indicate that it is likely that negative charges alone are not sufficient to enhance either the interaction of NS5A with the core protein or virus production.

Subcellular localization of NS5A and core protein in Huh-7 cells expressing HCV genomes. The coimmunoprecipitation experiments described above indicate that the wild-type NS5A but not the CL3B/SA mutant interacts with the core protein. To evaluate the NS5A-core protein interaction in intact cells, we examined the subcellular localization of NS5A with the core protein by immunofluorescence analysis. NS5A colocalized with the core protein in cells transfected with the JFH-1 wild type (Fig. 7A), whereas their colocalization was rarely observed in cells transfected with the CL3B/SA RNA (Fig. 7B).

To further analyze the subcellular compartments for the localization of NS5A and core protein in cytoplasmic membrane structures, including the endoplasmic reticulum (ER) and LDs, we performed subcellular fractionation studies as